CHARLES UNIVERSITY IN PRAGUE
Faculty of Science

Liquefaction phenomenon in Geotechnical Engineering

DIPLOMA THESIS

Hana Šantrůčková

Prague, 2009

CHARLES UNIVERSITY IN PRAGUE
Faculty of Science
Institute of Hydrogeology, Engineering geology & Applied Geophysics

Liquefaction phenomenon in Geotechnical Engineering

DIPLOMA THESIS

Hana Šantrůčková

Supervisor: Dr. David Mašín

Technical Supervisor: Prof. Pierre Foray

Prague, 2009

UNIVERZITA KARLOVA V PRAZE, PŘÍRODOVĚDECKÁ FAKULTA
Ústav hydrogeologie, inženýrské geologie a užité geofyziky

Ztekucení zemin v geotechnickém inženýrství

DIPLOMOVÁ PRÁCE

Hana Šantrůčková

Vedoucí: Dr. David Mašín

Odborný vedoucí: Prof. Pierre Foray

Praha, 2009

Acknowledgement

I would like to thank my supervisor David Mašín for encouraging me throughout my studies in Prague and Grenoble. Thanks to his involvement I had the possibility of experiencing studies abroad, which opened a PhD position in Laboratory 3S-R (Laboratoire Sols Solides Structures-Risques) in Grenoble. His critical reading of my manuscript was very valuable and his remarks gave me new inspiration for future progress.

I would also like to give my thanks to Pierre Foray, who had been supervising my practical work on my thesis. His knowledge is an inspiration for me and I'm looking forward to our future cooperation.

Last but not least thanks goes to my family and friends who supported me throughout my studies.

Abstract: The phenomenon of cyclic soil liquefaction is widely studied, but yet not well understood. The great concern of liquefying soils is the potential impact on structures and their stability. Apart from introducing liquefaction phenomenon, aim of this report is to present an evaluation of liquefaction potential for a site *Belle Plaine*, located in Guadeloupe. For this purpose, laboratory 3S-R (Laboratoire Sols Solides Structures-Risques) preformed three piezocone tests (CPTU) and installed four pore pressure sensors on the site of Belle Plaine. The obtained measurements were subsequently analyzed for liquefaction potential, which forms the main subject of this report. The interpretation of soil profile is based on general evaluation of CPTU readings, dissipation tests and on classification charts. According to these, Belle Plaine profile is divided into different soil horizons with sand layer and clay layer representing main two soil types. Subsequent evaluation of liquefaction potential is done according to semi-empirical methods by Seed and Robertson and by classical graphical evaluation methods. As a result, the Belle Plaine site is claimed to be potentially liquefiable from depth of 2.5 to 8 meters. This liquefiable horizon is formed by very fine clean sand with possible addition of fines in transition zones (i.e. zones where one soil type verges into another). Second part of the report deals with simplified modeling of seismic response of Belle Plaine site. This is done in order to compare earthquake loading predicted by a numerical code PLAXIS Dynamic with earthquake loading obtained traditionally from an equation by Seed and Idriss (1971). The results were used to redefine the factor of safety for Belle Plaine site and a comparison between empirical and numerical results was made.

List of Figures and Tables:

PART I – INTRODUCTION

The phenomenon of cyclic soil liquefaction is widely studied, but yet not well understood. The great concern of liquefying soils is the potential impact on structures and their stability. Aim of the following report is to not only introduce current knowledge concerning liquefaction phenomenon, but mainly to present a case study evaluating liquefaction potential for a site *Belle Plaine*.

Part II of this report introduces main principles of liquefaction phenomenon and methods for evaluating liquefaction potential. Furthermore, solutions for construction on liquefiable soil are presented. Liquefaction phenomenon is commonly divided into two separate mechanisms – Flow liquefaction and Cyclic mobility. These mechanisms are described in more detail in sections 1.2 and 1.3. Criteria such as historical, compositional, state and geologic criteria help to determine whether soil is or is not susceptible to liquefaction. Understanding the state criteria is necessary for understanding mechanisms leading to soil liquefaction. Current geotechnical practice uses several methods for evaluating liquefaction potential of soil. The most commonly used methods such as Seed cyclic stress approach and Robertson analysis are presented. When a site is evaluated as potentially liquefiable but is nevertheless destined for construction, there are two main ways how to approach this task. Either the foundation elements of a structure are designed to resist the effects of liquefaction or the soil characteristics are modified in order to decrease the risk of liquefaction. These different ways of approaching the problem of constructing on liquefiable soil are described in last section of Part II of this report.

A case study evaluating liquefaction potential of *Belle Plaine* site is summarized in Part III of this report. Belle Plaine site is located on the southern coast of the Grande-Terre Island, which is one of the islands forming Guadeloupe territory. Laboratory 3S-R (Laboratoire Sols Solides Structures-Risques) was dealing with determination of liquefaction potential for Belle Plaine site from *in-situ* tests. For this purpose, laboratory 3S-R preformed three piezocone tests (CPTU) and installed four pore pressure sensors on the site. The obtained measurements were subsequently analyzed for liquefaction potential, which forms the main subject of this report. The interpretation of soil profile is based on general evaluation of CPTU readings, dissipation tests and on classification charts. According to these, Belle Plaine profile is divided into different soil horizons with sand layer and clay layer representing two main soil types. Subsequent evaluation of liquefaction potential is done according to semi-empirical methods by Seed and Robertson and by classical graphical evaluation methods. As a result, the Belle Plaine site is claimed to be potentially liquefiable from depth of 2.5 to 8 meters. This liquefiable horizon is formed by very fine clean sand with possible addition of fines in transition zones (i.e. zones where one soil type verges into another).

Part IV of the report deals with simplified modeling of seismic response of Belle Plaine site. This is done in order to compare earthquake loading predicted by a numerical code PLAXIS Dynamic with earthquake loading obtained traditionally from an equation by Seed and Idriss (1971). The results were used to redefine the factor of safety for Belle Plaine site and a comparison between empirical and numerical results was made.

The presented report is a summary of work and research done in the field of liquefaction and liquefaction potential analysis. Parts III and IV were completed under the supervision of Pierre Foray from the *Géo* department in Laboratoire 3S-R, Grenoble.

PART II – LIQUEFACTION

1 Introduction

Liquefaction is a complex phenomenon which is caused by excess pore pressure generation and subsequent loss of shear strength under undrained conditions. When soil performing contractant behavior is subjected to loading, it has a tendency for densification. If the soil is saturated and under undrained conditions, excess pore pressures increase and therefore effective stresses decrease. This process results in critically low effective stresses and the soil is said to have liquefied. Liquefaction phenomena are generally divided into two main categories (Kramer, S. L., Geotechnical Earthquake Engineering):

- Flow liquefaction
- Cyclic mobility

1.1 Flow Liquefaction

A very loose specimen subjected to loading in undrained triaxial test exhibits peak strength at small shear strain and subsequently collapses to large strains at low confining pressure (Kramer, 1996). This behaviour is referred to as flow liquefaction. Locus of points defining in p-q-e space when liquefaction is triggered is called flow liquefaction surface (Karmer, 1996).

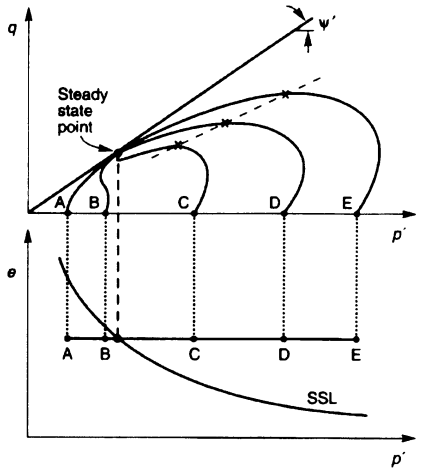

Figure 1 : Response of five specimens under monotonic loading. Specimens are consolidated to the same initial void ratio at different confining pressures. Because they have the same void ratio, they will reach the same effective stress conditions at the steady state. Each sample reaches the steady state by a different stress path. Flow liquefaction is initiated in specimens C, D and E at points (marked X) where a peak undrained strength is reached and the sample "collapses". Specimens A and B perform dilative behavior. (Kramer, 1996)

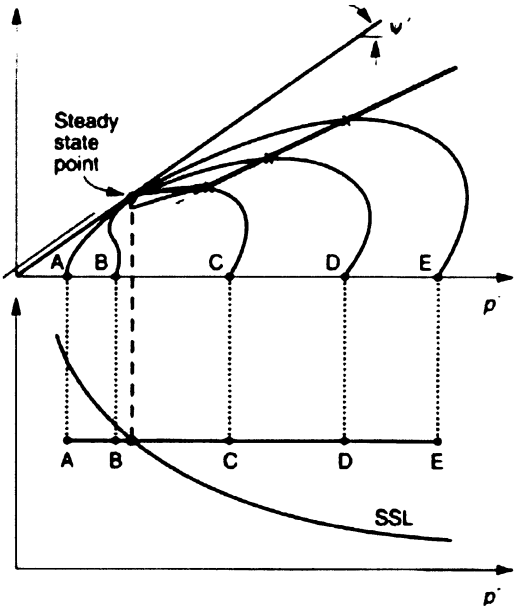

Figure 2 : Flow liquefaction surface (marked in color). Flow liquefaction cannot occur if stress path is below the steady state point (Kramer, 1996)

Flow liquefaction can be triggered by monotonic or cyclic loading. According to Kramer (1996), identical FLS can be applied to both monotonic and cyclic loading. In either case, when reaching the FLS, liquefaction is triggered.

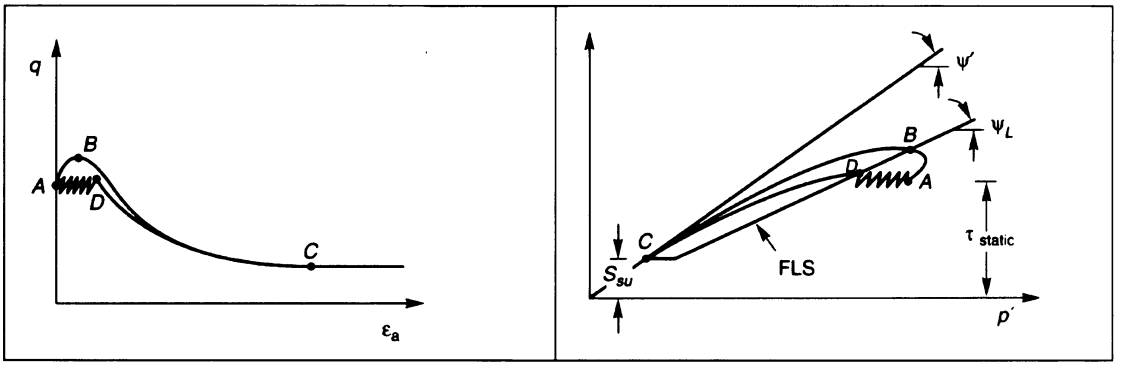

Figure 3 : Liquefaction initiation by monotonic and cyclic loading (Kramer, 1996)

1.2 Cyclic Mobility

Cyclic mobility is a phenomenon, when pore pressures in soil build up as a result of undrained cyclic loading. Consequently the effective stress reaches value close to zero. At this point, the soil

starts to behave as liquid and large deformations take place. The loss of strength due to cyclic undrained loading is plotted in Figure 4.

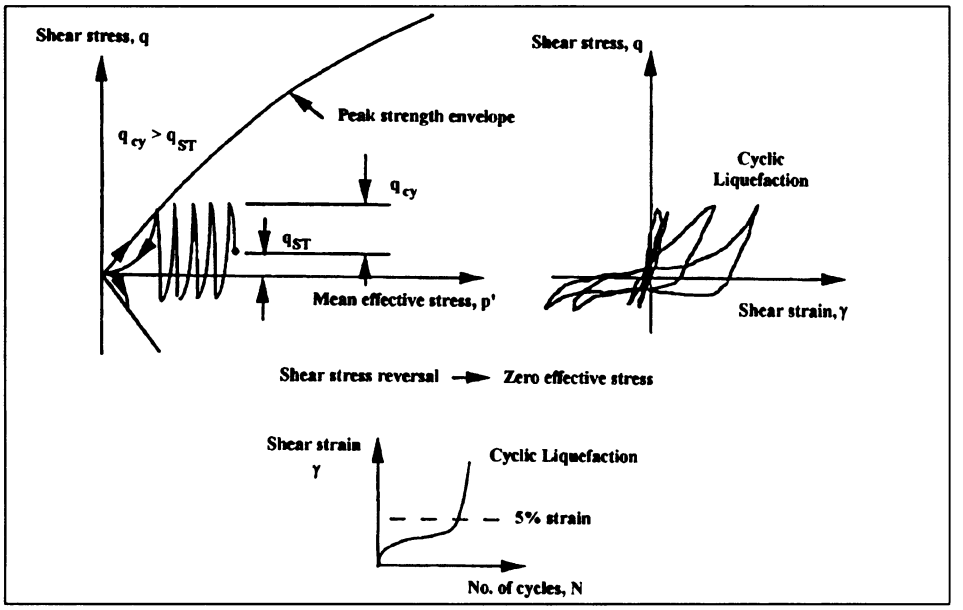

Figure 4: The loss of strength due to cyclic loading (after Robertson, 1994).

2 Liquefaction susceptibility

Understanding the nature of liquefaction phenomenon, it can be deduced that not all soils are susceptible to liquefaction. Kramer (1996) introduced several criteria which define liquefaction susceptibility of soils. These include *historical criteria, geologic criteria, compositional criteria* and *state criteria.*

2.1 Historical criteria

It has been shown that many liquefaction phenomena are often tied to a place where liquefaction has already occurred[1]. This observation is connected to the fact that liquefaction is commonly triggered by an earthquake motion, which often recurs at same areas (i.e. tectonically active areas). These observations provide information determining areas historically susceptible to liquefaction (for review see Kramer, 1996).

[1] This is valid in cases when groundwater conditions and soil characteristics have remained unchanged.

2.2 Compositional criteria

Liquefaction phenomenon is connected with soils having high contractant volume change potential. This fact can be deduced from the knowledge that soil liquefaction is caused by increasing excess pore pressures in undrained conditions. Volume change potential is influenced by different soil chracteristics:

- particle size
  - even though coarse-grained soils like gravel have a high volume change potential and perform contractant behavior, they are usually considered as non-liquefiable deposit because they are too permeable to generate high excess pore pressures[2]
  - fine grained soils like clays are generally thought to be non-liquefiable considering their dilatative behavior or stable contractive behaviour. Hence inability to generate high excess pore water pressures

- particle shape
  - soils with rounded particle shapes are able to densify more than soils with angular shapes therefore soils with rounded grains are more susceptible to liquefaction

- soil gradation
  - well graded soils are generally less susceptible to liquefaction because of their lower volume change potential

The effect of fine content on soil liquefaction is a very problematic issue and is not well understood at present. It used to be believed that cohesive soils are not susceptible to liquefaction but this was proved wrong by numerous authors (eg. Wang, 1979). Wang (1979) introduces four Chinese criteria which define fine-grained soils susceptible to liquefaction:

- Fraction finer than 0.005 mm $\leq$ 15%
- Liquid limit $\leq$ 35%

[2] this is not true for gravel under truly undrained condition; these conditions can be simulated in laboratory but are very rarely in the field, because of rare presence of fully impermeable layers that generate truly undrained conditions (reviewed in Kramer, 1996)

- water content more than 90% of liquid limit of soil
- Liquidity index ≤ 0.75

These criteria are widely known, although there exist many exceptions when soils not satisfying Chinese criteria liquefied (eg. Miura et al., 1995). For this reason further research has been carried out.

2.3 State criteria

2.3.1 Flow liquefaction

Liquefaction susceptibility of soil is strongly influenced by its initial stress and density. Based on his results from undrained triaxial tests, Castro (1969) defined a "steady state of deformation", i.e. a state when sand specimen deforms continuously under constant shear stress. This state can be viewed in σ' versus τ versus e space (Figure 5)[3] as a plane.

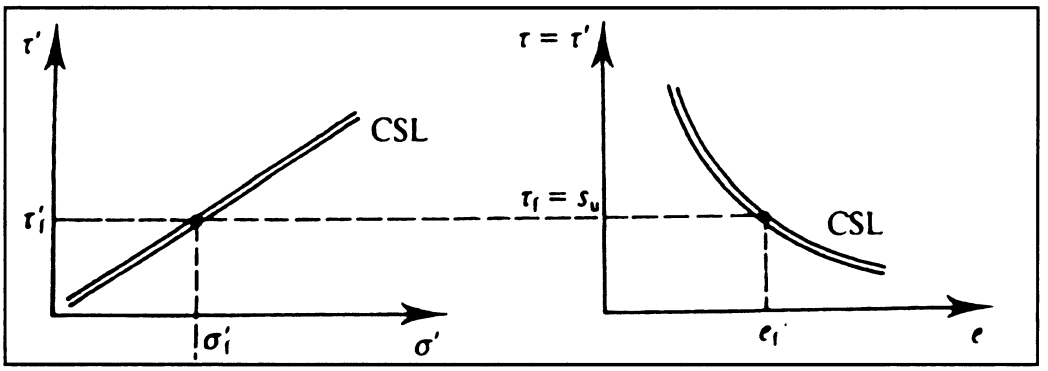

Figure 5: Critical state line (Atkinson, 1993)

Projecting steady state plane onto *log* σ_c versus e space, a steady state line (SSL)[4] is received. It was noted that soil whose state plots below the SSL is not susceptible to flow liquefaction (Figure 6). On the other hand, soil whose state plots above the SSL is susceptible to liquefaction only if the static shear stress exceeds its steady state (or residual) strength (Figure 6,7) (for review see Kramer, 1996).

[3] alternatively p' versus q' versus υ space

[4] SSL is commonly said to be have the same meaning as CSL (Been et. al, 1991)

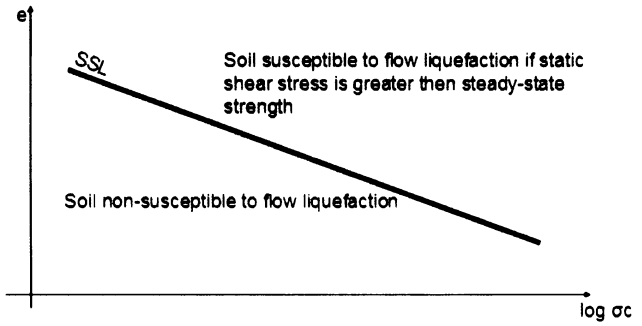

Figure 6: Steady state line (in blue) (modified from Kramer, 1996)

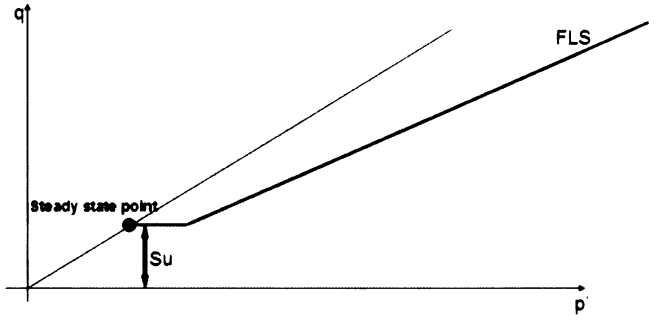

Figure 7: Zone of susceptibility to flow liquefaction, i.e. when initial static shear stress exceeds its steady state strength (su). Initial states that fall into the blue zone define liquefiable soils and liquefaction occurs when their undrained effective stress path reaches the FLS (modified from Kramer, 1996)

2.3.2 Cyclic mobility

Cyclic mobility, unlike flow liquefaction, can develop in soils whose state lies above or bellow the SSL, i.e. in loose and dense soils (Figure 8).

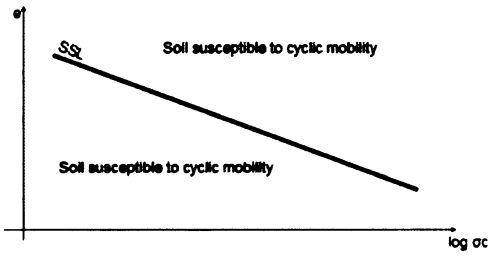

Figure 8: Cyclic mobility can occur in loose and dense soils (modified from Kramer, 1996)

Considering the stress criteria, cyclic liquefaction can occur when static shear stress is smaller than steady state strength (Figure 9) (for review see Kramer, 1996)

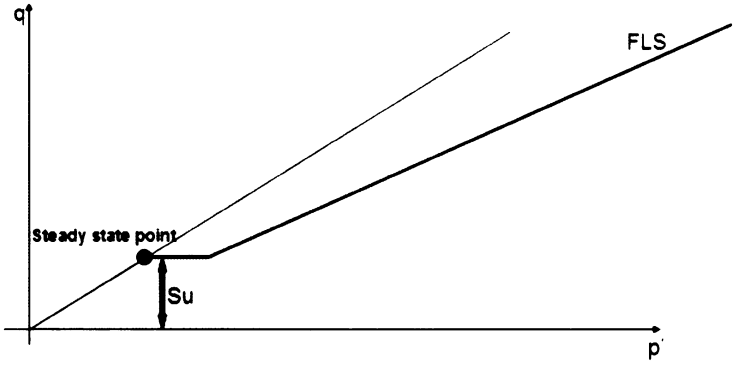

Figure 9: Cyclic mobility can occur when static shear stress is smaller than the steady state strength (su) (modified from Kramer, 1996)

Considering all previously mentioned criteria, one can make a rough judgment of soil susceptibility to liquefaction. In cases when liquefaction susceptibility has to be examined in more detail, there exist various empirical, numerical and graphical methods for liquefaction evaluation. Some of these are described in the following text.

2.4 Geologic criteria

These criteria define a range of geologic factors contributing to formation of soils susceptible to liquefaction:

- processes that sort soil into uniform grain size distribution (fluvial, aeolian deposits)
- deposition of soil into lose state (fluvial, aeolian deposits)
- high groundwater level making the soil saturated at low depths (liquefaction susceptibility increases with decreasing groundwater depth)
- young age of the deposit (Holocene deposits are more susceptible to liquefaction then Pleistocene deposits)

(for review see Kramer, 1996)

3 Methods used for liquefaction potential evaluation

There are many methods used for liquefaction potential evaluation. The following text introduces basic methods used in the current practice.

- Semiempirical methods:
  - Robertson method
  - Seed method
- Graphical methods:
  - Robertson chart
  - Bq versus qt chart

3.1 Seed method, cyclic stress approach

The main idea of this method is to compare earthquake loading with cyclic resistance of the soil. Earthquake loading can be expressed in terms of shear stresses and so can liquefaction resistance of soil. If cyclic shear stress induced by an earthquake exceeds shear stress expressing liquefaction resistance of the soil, liquefaction can be expected (for review see Kramer, 1996).

An earthquake induces cyclic loading, which is not uniform. Therefore, in order to be able to compare the two shear stresses (i.e. shear stress induced by an earthquake and shear stress expressing liquefaction resistance of the soil), a simplification is made - it is assumed, that the uniform cyclic loading amplitude is equal to 0.65 of maximal cyclic loading amplitude[5]:

$$\tau_{cyc} = 0.65\tau_{max} \qquad (1)$$

In geotechnical practice, τ_{max} is calculated after Seed and Idriss (1971) as

$$\tau_{max} = (a_{max}/g)\sigma_{vo}rd \ ^{6} \qquad (2)$$

[5] Earthquake induced loading can be predicted in two ways – detailed ground response or simplified approach (for review see Kramer, 1996). This work mentions only simplified approach, because going into more details is out of scope of this work.

[6] for review see Kramer, 1996

where a_{max} is peak horizontal acceleration and σ_v is total vertical stress. Component *rd* is a stress reduction factor with maximum value of 1. The following equation after Seed and Idriss (1971) describes *rd* as a ratio of cyclic stress for flexible soil column to cyclic stress for rigid soil column:

$$rd = (\tau_{max})_d / (\tau_{max})_r \quad [7] \qquad (3)$$

This uniform cyclic shear stress τ_{cyc} is applied for a number of cycles that induce the same pore pressure increase as the irregular time history of real earthquake. Number of uniform cycles increase with increasing earthquake magnitude and this correlation is shown in Table 1.

Magnitude	Number of Cycles
5.25	2-3
6	5
6.75	10
7.5	15
8.5	26

Table 1: Number of equivalent uniform stress cycles for earthquakes of different magnitude (Idriss, 1999)

Liquefaction resistance determination can be based on laboratory tests or *In Situ* tests (for review see Kramer, 1996). The following text mentions only a method used for liquefaction resistance evaluation from cone penetration test (CPT). [8] Readings from cone penetration test provide values of tip resistance. Using normalized values of cone resistance and CPT-based liquefaction curves (Figure 10), minimum cyclic stress ratio at which liquefaction is expected can be determined. Minimum cyclic stress ratio required to initiate liquefaction increases with decreasing earthquake magnitude. Figure 10 presents liquefaction curves for a magnitude of 7.5, but cyclic stress ratio for other magnitudes can be obtained by multiplying the cyclic stress ratio for magnitude 7.5 by factors presented in Table 2.

Magnitude	$CSR_M/CSR_{7.5}$
5.25	1.5
6	1.32
6.75	1.13
7.5	1
8.5	0.89

Table 2: Magnitude Correction Factors ffor Cyclic Stress Approach (Kramer, 1996)

[7] for review see Idriss et al.,2004

[8] This is because detailed description of liquefaction evaluation methods is out of scope of this work.

Cyclic stress approach defines earthquake loading by uniform cyclic shear stress amplitude applied for a certain number of cycles. Liquefaction resistance is characterized by amplitude of uniform cyclic shear stress inducing liquefaction in the same number of cycles. Having cyclic stress ratio initiating liquefaction and comparing it to cyclic stress ratio induced by the earthquake, factor of safety is obtained (for review see Kramer, 1996):

$$FS = \tau_{\text{required to cause liquefaction}} / \tau_{\text{induced by an earthquake}} = \tau_{cyc,L} / \tau_{cyc} = CSR_L / CSR^{9} \qquad (4)$$

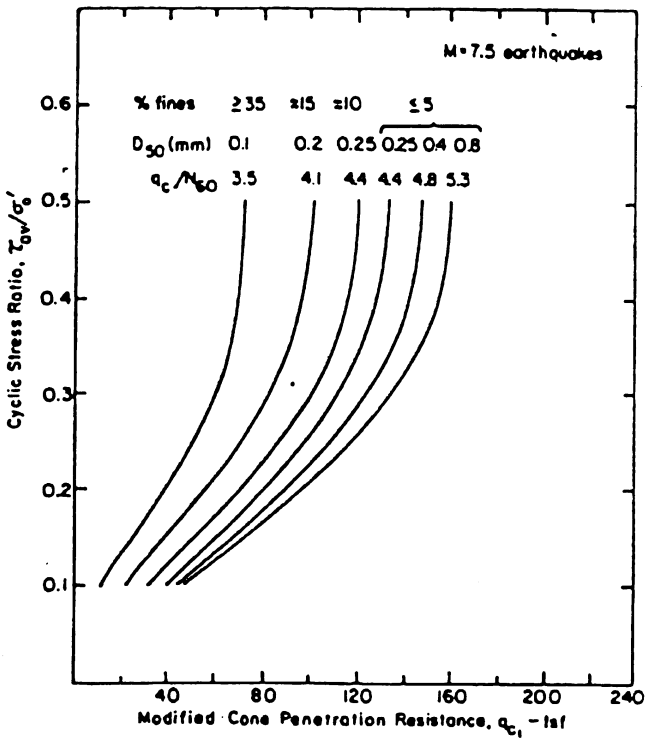

Figure 10: Stress ratio causing liquefaction versus cone resistance; relationship is plotted for sands with different fine content (after Seed and De Alba; 1986)

3.2 Robertson analysis

Robertson analysis represents another method of liquefaction evaluation based on CPT data. In this method, the evaluation of cyclic stress ratio at which liquefaction is expected is not done as in the Seed method, but is done according to chart shown in Figure 11. It can be seen that Robertson

[9] $CSR_L.\sigma'_{vo} = \tau_{cyc,L}$

incorporates the calculation of fine content and soil type evaluation (i.e. Ic evaluation) in the process of calculating the liquefaction stress ratio, which means that the value of resulting ratio is already influenced by the effect of fine content and sensitivity of soil.

The cyclic stress ratio of an earthquake is calculated in a same way as in Seed method.

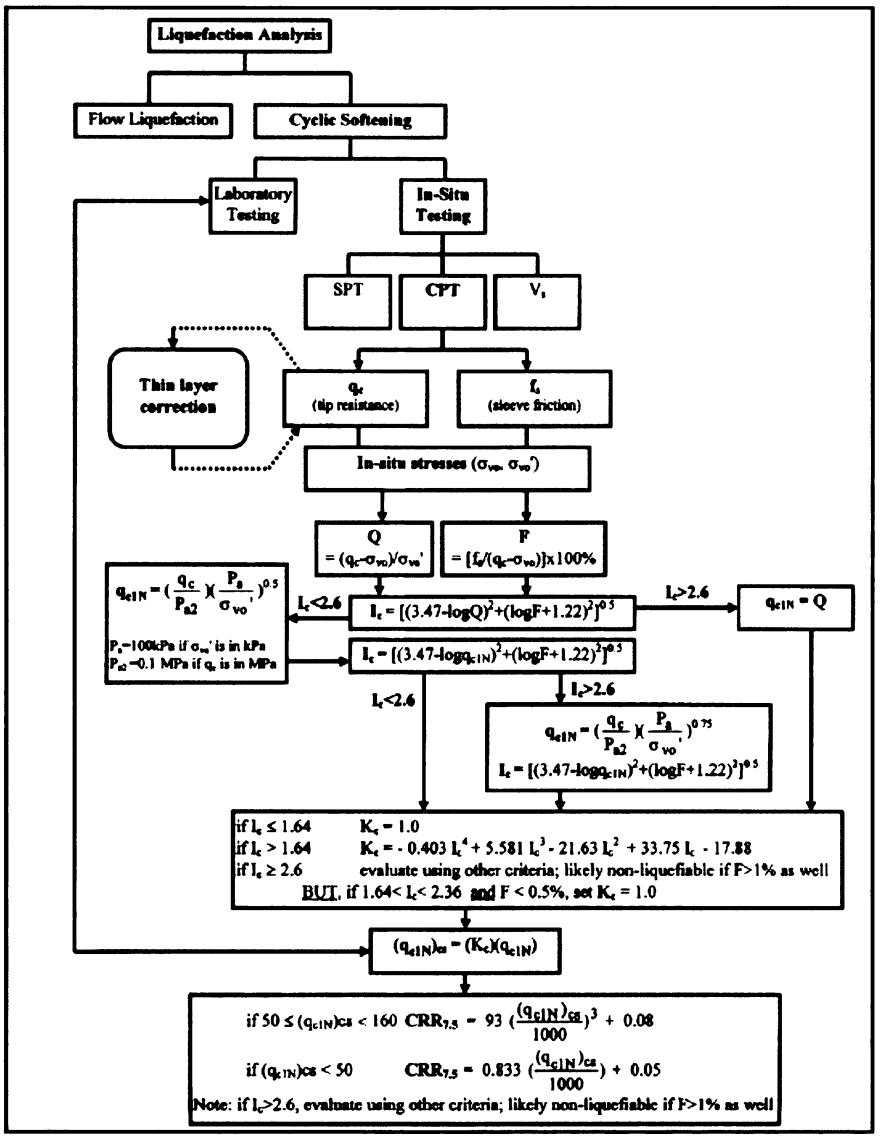

Figure 11: Flow chart explaining the used evaluation of liquefaction potential based on CPT data (Robertson, 1998)

3.3 Graphical methods:

Liquefaction potential can be also evaluated by use of graphical methods. Two graphical methods are presented and subsequently used in Part III/section 4 of this work.

- Robertson chart: This chart (appendix D) is separated into three zones. *A zone* corresponds to soils, which are susceptible to cyclic liquefaction. *Zone B* refers to soils with soil behavior type index Ic>2.6 (Table 3) and normalized sleeve friction ratio[10] F>1%, that means likely non-liquefiable. Soils with Ic>2.6 and Fr<1% may be potentially liquefiable due to the sensitivity of the soil. These soil types are marked by *zone C*.

Ic<1.31	Gravelly sand to dense sand
1.31<Ic<2.05	Sands: clean sand to silty sand
2.05<Ic<2.6	Sand mixtures: silty sand to sandy silt
2.6<Ic<2.95	Silt mixtures: clayey silt to silty clay
2.95<Ic<3.6	Clays:silty clay to clay
Ic>3.6	Organic soils: peats

Table 3: Soil behavior type index Ic is a function of normalized CPT resistance and of normalized friction ratio. Its value characterizes the soil type (for review see Robertson and Wride, 1998)

- Bq versus qt chart: This chart (appendix D) highlights zones, where soil is potentially liquefiable. It is based on the effect of pore pressures on soil liquefaction.

4 Construction on liquefiable soil and ground improvement methods

4.1 Introduction

Areas susceptible to liquefaction are sometimes destined for construction. The main reasons for building on a liquefiable site are favorable location and space restrictions. There are two main ways how to approach this task:

- Foundation elements of a structure are designed to resist the effects of liquefaction.
- Soil characteristics are modified in order to decrease the risk of soil liquefaction – ground improvement methods.

[10] Sleeve friction ratio F is a normalized value of CPT sleeve friction stress. Friction stress is increasing with fine content in soil.

4.2 Liquefaction resistant structures

Large soil deformation and differential settlements affect a structure when constructed on a liquefied layer. As a result, the structure can undergo sinking, tilting or total collapse. To ensure the structure safety, special design approaches should be implemented.

4.2.1 Shallow Foundations

Unfortunately there is no general engineering method for evaluating behavior of shallow foundations for a wide range of soil, foundation and earthquake parameters (Liu and Dobry, 1997). Yet there exist field studies on foundation damage due to liquefying soil. These observations show that structure stability depends on foundation parameters, structure parameters and also on effects of adjacent structures. The effect of adjacent structures can be explained by the fact that excess pore pressures generated by shaking are smaller under a foundation than in the free field (for review see Liu and Dobry, 1997). The presence of surrounding structures inducing extra load on the soil makes the area less susceptible to liquefaction, therefore more stable. This theory was proved right by a field study (Tokimatsu et. al, 1991) carried out in Daugupan City, Philippines after occurrence of an earthquake in 1991. It was shown that most significant settlements were observed in buildings without adjacent structures or in buildings surrounded by light weight structures.

Design factors affecting behavior of shallow foundations build in liquefaction susceptible areas:

- Structure having all foundation elements tied together exhibits less differential settlements because its foundation moves uniformly and loads from locally liquefied zones can be transferred to adjacent stronger areas. Therefore continuous footings such as mat foundations or footing tied together by grade beams are often used for buildings on liquefiable foundation soils. Although it has to be noticed that continuous foundations prevent differential settlements but are susceptible to tilting and overturning (Liu and Dobry,1997)
- Experimental data (Figure 12 – Yoshimi and Tokimatsu, 1977) and field data (Figure 13 – Lee and Dobry 1997) show that width of a foundation built on liquefying sand corresponds to its settlement. Figures 12, 13 demonstrate that foundation settlement increases with decreasing width of the foundation.

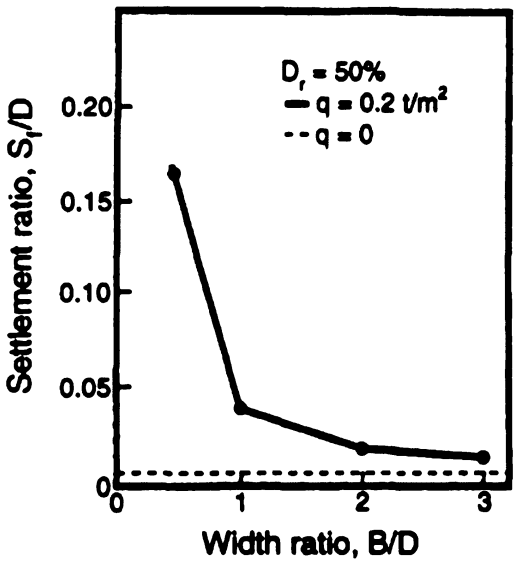

Figure 12: Results of laboratory testod model foundation on liquefiable sand (Yoshimi and Tokimatsu, 1977)

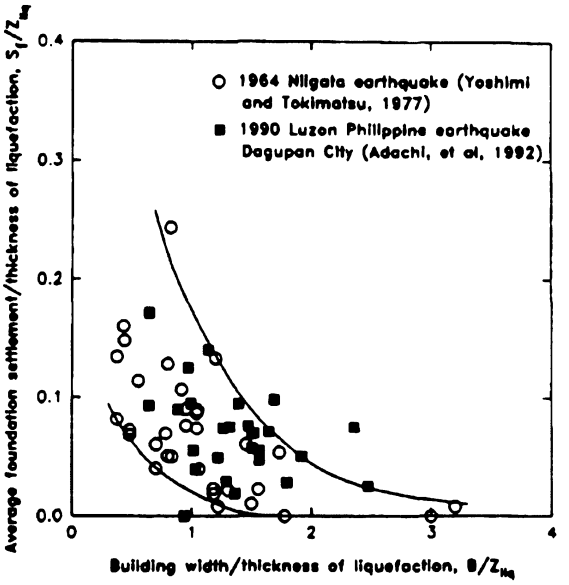

Figure 13: Normalized Foundation Settlement versus Normalized Building width (Liu and Dobry, 1997)

4.2.2 Deep Foundations

4.2.2.1 Introduction on behavior of pile in liquefiable soil

Pile is designed as a slender column with lateral support from the surrounding soil. As soil liquefies, it loses its shear strength and the pile foundation becomes less supported. The subsequent

flow of liquefied soil imposes a bending moment on the pile. These mechanisms can cause the pile to fail due to its insufficient resistance (Bhattacharya et al., 2003).

A common method currently used for design of piles in liquefying soil is a "force limit analysis". This method is used in several design codes (JRA 1996 – Japanese Highway code of practice; NEHRP 2000 – USA code; Eurocode 8) and is based on estimation of lateral pressure acting on the pile body and evaluation of the pile response (Puri and Prakash, 2008). This method of analysis assumes that lateral pressure applied by a liquefied layer on a pile is 30% of total overburden pressure[11] (Figure 14). Due to lateral spreading of the soil, bending moments are generated. These bending moments have a maximum value between the liquefied and non-liquefied soil layer (Puri and Prakash, 2008).

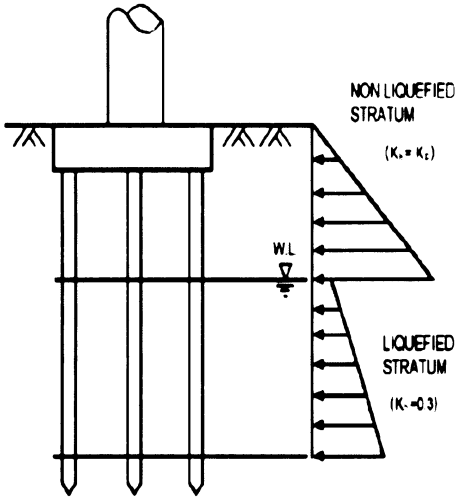

Figure 14: Lateral pressure distribution (for review see Puri and Prakash, 2008)

The method of "force limit analysis" was criticized for its inconsistency in a paper by Bhattacharya et al. (2003). Their work mentions a case study of Showa Bridge destruction after Niigata Earthquake which occurred in 1964. The destruction of Showa Bridge was widely accepted to be due to lateral spreading failure[12]. Considering this point of view, Bhattacharya (2003) posed following questions:

- Why did the piers deform in different directions when lateral spreading should cause identical deformation of the piers.
- Why are there some piles experiencing biggest deformation due to lateral spreading in an area which is not the interface of liquefiable and non-liquefiable layer?

[11] This estimation is based on back calculation

[12] "Lateral spreading failure" is referred to when soil liquefies, loses its shear strength and flows while dragging the pile with it.

As a solution, the paper proposes a new hypothesis of a failure. This suggests that pile may lose its stability even before the onset of lateral spreading and this is for the following reason: Soil liquefaction causes the soil to lose its shear strength and therefore the soil no longer offers a sufficient support to the pile. The pile doesn't sustain the axial load and buckles sideways in a direction of least bending elastic stiffness (Bhattacharya,2003) end eventually may lose its stability. This mechanism may be supplemented by lateral loads due to horizontal movement of the soil.

The previous text and the fact that pile instabilities occur even though piles are designed with sufficient resistance suggest that further research is needed. Although it has to be noted, that this section doesn't fully cover the current knowledge on pile instabilities in liquefied soil. This is because detailed report on pile behavior and pile design in liquefied soils is out of scope of this work.

4.2.2.2 How to provide sufficient pile resistance

Some factors increasing the pile resistance against effects of liquefied soil:

- Designing a pile foundation according to design codes with a sufficient factor of safety
- Designing a joint between the pile and its head in a ductile manner. As a consequence some rotation of the joint is allowed.
- Constructing a pile of bigger dimensions and larger amount of reinforcement

4.3 Soil Improvement

There exist certain criteria which identify a soil more susceptible to liquefaction and a soil less susceptible to liquefaction (Table 4). The essential condition for soil to liquefy is that it has to be saturated.

Criteria increasing liquefaction susceptibility	Criteria decreasing liquefaction susceptibility
- Uniform grain size distribution - Poor gradation - Lose state of the deposit - Young age of the deposit (Holocene age) - High volume change potential	- Increasing ground water depth - Low ability to produce high excess pore pressures - Angular shape of grains

Table 4: Criteria effecting liquefaction resistance

Table 4 demonstrates that there exist certain conditions and soil properties that prevent the soil from liquefying. This fact led to an idea that modification of soil properties could reduce the risk of liquefaction and associated ground deformation. In current practice, liquefiable foundation soils are generally treated before being built on. This treatment can be of different nature (Andrus and Chung, 1995):

- **Soil densification** - there is a direct correlation between soil density and volumetric change potential: densification of soil decreases soil volumetric potential and therefore decreases liquefaction susceptibility
- **Solidification** - gives a cohesive strength to soil and prevents grain movement
- **Drainage** - decreases level of saturation, which is an essential condition for liquefaction
- **Reinforcement**: provides resistance to ground deformations

Factors affecting the choice of soil improvement technique are (Moffat, 2008)

- impact to the environment
- structure type
- settlement tolerances
- soil permeability
- cost

Following text briefly introduces some of the common technologies of soil improvement.

4.3.1 Vibro-compaction

Vibro-compaction is a popular method of improving granular, non-cohesive foundation soils. Vibration probe is penetrated into the ground using water flush and performs horizontal vibrations, which cause grain structure of soil to collapse. During this state, material (e.g. sand) can be added into the puncture and compacted into collapsed structure of soil (Figure 15). Vibration probe is penetrated into the ground in a grid pattern and can affect areas up to 30 meters depths (Moffat, 2008)

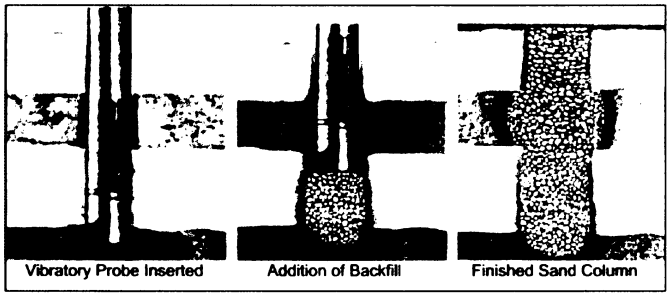

Figure 15: Soil compaction by vibroflotation method (Moffat, 2008)

4.3.2 Stone columns

Stone columns are compacted gravel bodies installed in a foundation soil for the purpose of its improvement. There are two most common methods used to construct stone columns (Adalier and Elgamal, 2004):

- Vibro-replacement
- Auger-casting system

Vibro-replacement (Figure 16) is a technology when vibration probe is penetrated into ground by vibration and water or air jetting. The hole is subsequently filled with gravel, which is inserted through a surface annulus or from the bottom of vibration probe. Vibrations and vertical movement of the vibration probe cause the gravel backfill (and possibly its surrounding) to densify and compact.

Relative density of surrounding soil having fine content less than 15% and clay content less then 2% is effectively increased by vibration (Adalier and Elgamal, 2004). Soils with more silt or clay content are not very affected by vibrations and the ground improvement process considers only the effect of soil replacement.

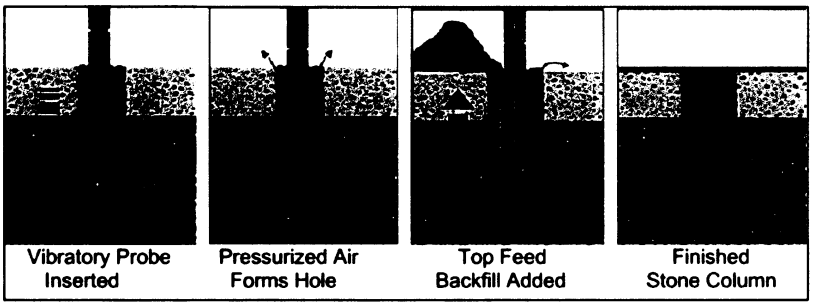

Figure 16: Stone column construction using vibro-replacement method (Moffat, 2008)

Another technology of stone column construction is an auger-casting method (Figure 17). A continuous auger is drilled into the ground and subsequently pulled out with simultaneous bottom gravel feeding (i.e. puncture is filled internally from auger tip). This method can be extended for a compaction rod system, which adds the effect of desinfication (Adalier and Elgamal, 2004).

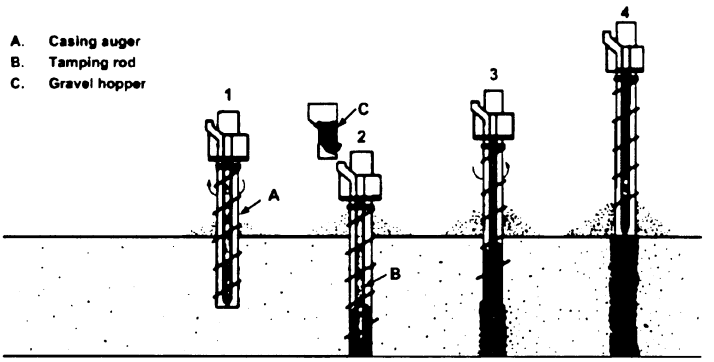

Figure 17: Stone column installation by the use of auger-casing method (for review see Adalier and Elgamal, 2004)

Stone columns increase total shear strength of the foundation soil, provide reinforcement, enable better drainage of soil layer and possibly increase relative density of the surrounding soil. These factors decrease the potential of liquefaction. Resulting level of improvement can be tested by SPT and CPT methods, pressuremeter tests and dilatometer tests.

Stone columns are widely used as a liquefaction countermeasure thanks to their effectiveness, low costs and suitability for urban areas[13].

4.3.3 Dynamic compaction

Decreasing the risk of liquefaction can also be achieved by applying dynamic compaction. This technique is based on dropping a heavy weight onto the ground which causes the soil to densify and settle. A disadvantage of this method is its aggressiveness which makes it impossible to apply dynamic compaction in areas adjacent to existing structures.

4.3.4 Compaction Grouting

This soil improvement method is often used for foundation soil bellow an already existing building. The technology enables to inject a low mobility grout[14] into the soil. This grout remains in a

[13] Unlike other improvement technologies (such as dynamic compaction), stone columns produce no significant vibrations or noise (Adalier and Elgamal, 2004)

homogenous mass and doesn't permeate through the soil grains (Andrus and Chung, 1995). As the grout mass expands, the soil is displaced and densified. As a consequence, the soil becomes more resistant to liquefaction.

There is number of factors influencing the effectiveness of compaction grouting (Andrus and Chung, 1995):

- Soil characteristics
- Grout mix
- Grout injection volume, pressure and rate
- Grout hole spacing

4.3.5 Permeation Grouting

This technology is based on injecting chemical[15] or particulate[16] fluid into grain structure of soil. The injected medium cements the soil particles together, strengthens the soil and therefore prevents the soil from high volume changes (Andrus and Chung, 1995). Factors influencing the effectiveness of permeation grouting are same as those listed in section 4.3.4.

4.3.6 Drainage techniques

Soil saturation is a substantial condition for liquefaction and therefore increasing drainage ability of soil can be a way of eliminating liquefaction phenomenon. Common drainage methods include drain installation (gravel drains synthetic drains), deep pumping, pressure relief wells[17], etc.(Moffat, 2008). Drainage techniques are often used as an addition to other soil improvement technologies.

[14] mixture of cement, water, sand

[15] e.g. sodium silicates

[16] mixture of Portland cement, clay, water

[17] Pressure relief well refers to vertical well constructed from material enabling water access but disabling entrance of solid particles into the well. A common purpose of these wells is relieving excess hydrostatic water pressures.

PART III – CASE STUDY: LIQUEFATION ANALYSIS OF *BELLE PLAINE* SITE

1 Introduction

Soil liquefaction caused by cyclic loading is a phenomenon widely studied, but yet not well understood. It used to be believed, that potentially liquefiable are only sands and sandy soils found in depositional areas of low altitudes. Occurring earthquakes bring surprising cases of liquefying silty profiles in the very heart of Mexico plateau (Mendoza, 1999). The lack of knowledge initiates new research projects with an ambition to extend our understanding.

1.1 Belle Plaine project

Study of soil liquefaction for real conditions is subject of a current project covered by BRGM – Service Aménagement et Risques Naturels (ARN). The investigated site is located on Grande-Terre Island in The Caribbean. This island belongs to a group of islands which together form Guadeloupe, an overseas department of France. The site of interest will further on be referred to as *Belle Plaine.*

Five major partners cooperating on an ANR (Agence Nationale de la Recherche) project are:

- ANTEA
- CERMS (Centre d'Enseignement et de Recherche en Mécanique des Sols)
- 3S-R (Laboratoire des Sols, Solides, Structures-Risques)
- LGIT (Laboratoire de Géophysique Interne et Tectonophysique)
- LMSS-Mat (Ecole Centrale Paris/Laboratoire de Mécanique des Sols, Structures et Matériaux)

Laboratory 3S-R deals with a task of evaluating soil liquefaction potential from *in-situ* methods. For this purpose, cone penetration tests and pore pressure measurements were carried out on the site. The data were subsequently interpreted and evaluated for liquefaction potential. Obtained findings make the subject of part II of this report.

1.2 Site Description

The investigated area lies on the southern coast of the Grande-Terre Island and is surrounded by mangrove vegetation. Tests carried out by laboratory 3S-R on the site were situated next to a sewerage plant where a data acquisition system was installed and which served as a storage place in

case of bad weather conditions. Photos and situation layout (Figure 18; Figure A1.1; Figure A1.2) give a closer view on the site and show the position of three preformed penetration tests (BP1/2; BP3; BP4) and four installed pore pressure sensors (PZ1-PZ4) (Figure 19).

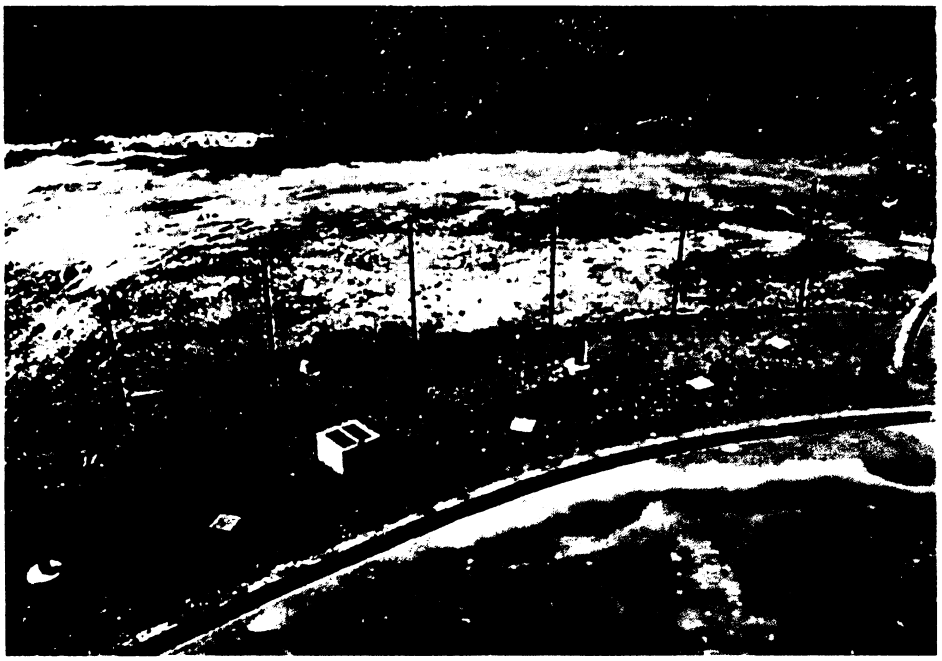

Figure 18: Photo taken at the Belle Plaine site; pore pressure sensors are placed between the fence and road, cone penetration tests were preformed behind the fence

1.3 Piezocone Test (CPTU) performed at Belle Plaine

Laboratoire 3S-R carried out cone penetration tests with additional pore pressure measurements (CPTU). These tests are becoming more and more popular in site investigation procedures. This is due to:

- Low costs and relatively reliable results
- Possibility of obtaining continuous information throughout the profile
- Pore pressure measurements
- Possibility of running dissipation tests while performing the penetration
- Compared do SPT, CPT has better detection of thin layers in stratigraphy of a soil profile

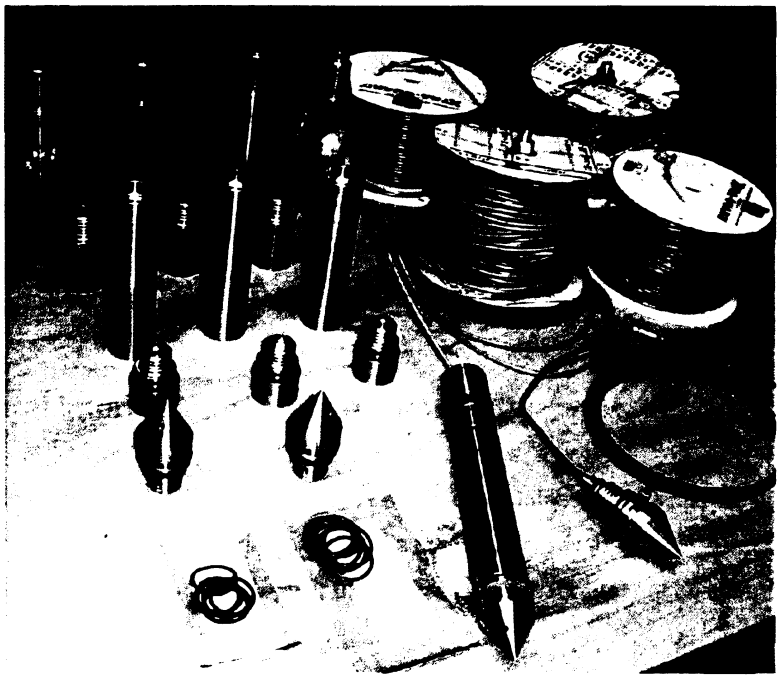

Figure 19: Pore pressure sensors used at Belle Plaine site

Three penetrometer tests were preformed at the Belle Plaine site. Cone penetrometer was pushed into the ground with constant rate of approximately 2cm/s. The pushing was discontinuous due to adding of new rods, which was done every meter. The signal containing all collected data was transmitted via a cable which led through rods to the surface.

Forces applied to the penetrometer by surrounding soil were measured by strain gauged load cells. The force acting on the cone *(Qc)* was divided by area of the cone and this gave a resulting *qc*, so called cone resistance. The force acting on a sleeve of the penetrometer was divided by area of the friction sleeve and this gave a value of *fs*, so called sleeve friction. Pore pressure was measured throughout the penetration and measurements were made behind the cone (u_2) (Figure A1.3). The pore pressure measuring system consists of pore pressure sensor located in the water chamber. This chamber communicates with soil in its surrounding by a porous filter and this way the liquid chamber is able to simulate the same water pressure as is in the pores of the surrounding soil. In addition to these measurements, three seismic sensors were added to the piezocone. The purpose of the seismic measurements was to obtain a small shear strain modulus (*Go),* which is essential for evaluation of soil motion induced by the earthquake. During the phase of putting additional rods, shear waves were produced by hammering on the surface. Geophones register the arrival time at different depths.

2 Interpretation of stratigraphy and soil classification:

The soil classification and strafigraphy interpretation was done by three methods.

- The general interpretation of readings obtained from CPTU
- Interpretation of dissipation tests
- Classification charts

2.1 General interpretation of measured data:

As a result of CPTU readings, three sets of data were obtained – qc, fs and u2. These data have to be corrected and normalized in order to perform a correct interpretation.

Due to technical reasons, the arrival time of seismic signal could not be interpreted[18]; therefore Vs and Go could not be evaluated.

2.1.1 Data correction

qc correction:

Mistake in qc readings was firstly observed for measurements done under water where the resulting cone resistance was not equal to underwater pressure. This difference was found to be caused by pore water pressure, which acts on the joints of penetrometer and influences the cone resistance and the friction sleeve measurements (for review see Powel and Lunne, 2005). In CPTU, the pore pressure measured "inside" the penetrometer also affects the penetration readings. This is called an"uneven area effect". A way to eliminate this effect is by correcting the tip resistance:

$$qt = qc + u_2(1-a) \qquad (5)$$

where a is an area ratio, which is roughly equal to a ratio of cross section of the area of load cell (net area) AN and projected area of the cone AT (total area) – Figure B1.1

[18] It is assumed, that vibrations caused by a machine at the surface affected the registered signal.

This correction is especially important for clays and silty soils, where the pore pressures may be very high with respect to low values of qc and so have a big influence on the results.

fs correction:

As friction sleeve is also exposed to pore water pressure effects, correction should be done for this area as well. There are empirical ways how to correct the results, but for this purpose, pore pressure behind the friction sleeve *(u3)* should be measured. If there are no readings of *u3* available, it is recommended not to do the correction (Lunne et al., 1997).

Because measurement behind the friction sleeve *(u3)* were not preformed for the Belle Plaine project, *fs* value is used without a correction.

2.1.2 Data normalisation

Measured values of cone resistance *qc* and sleeve friction *fs* are highly influenced by confining pressure, therefore by the effective overburden stress. For example, values of tip resistance and sleeve friction measured at great depths are increased by the high value of confining pressure. On the contrary, CPT readings for shallow depths are reduced by the low values of confining stress (1). In order to compare and evaluate the measured results, there is a need to normalize the tip and sleeve resistance to a reference value. For this reason, a value of one atmosphere[19] was introduced as a reference stress value and is used in the current practice (1).

Extensive research was done on the subject of data normalizing, coming with numerous methods and procedures. Applying a correct normalization to each type of soil is a complicated procedure to undertake in general practice. That's why the following simplified normalization equation was introduced (Lunne et al., 1997):

- Normalised net tip resistance: $Qc = (qc - \sigma_{vo})/\sigma'_{vo}$ *(6)*

- Normalised sleeve resistance: $Fr = fs/(qt-\sigma_{vo})$ *(7)*

where σ_{vo} is vertical overburden stress; σ'_{vo} is effective vertical overburden stress; *qc* is cone resistnce and *fs* is sleeve friction

[19] 1 atmosphere = 101.325kPa

2.1.3 Data interpretation based on qt, Rf and u_2:

- Corrected tip resistance profile qt signalizes layers of soft clayey soils by low values and sandy soils by higher values. Very low values of cone resistance are typical for organic soils.

- Friction ratio Rf is a ratio of sleeve friction and cone resistance. Because sleeve friction rises with fine particle content, Rf is higher in clayey soils then in sandy soils. Very high values of friction ratio are typical for organic soils. The relation between cone resistance and friction on the sleeve is shown in Figure B1.2.

- Each soil type reacts differently to pressure applied by the cone. The volume change of pores can be interpreted from the pore pressure measurements, therefore different layers of soil type can be recognized from u_2 readings. Measured pore pressures in normally consolidated clean sand often coincide with hydrostatic pore pressure. This is because NC clean sand is very permeable. On the contrary, measured pore pressures in normally consolidated clays can rise to very high values. This is because of the low permeability and contractant behavior of NC clays. Therefore when pore pressure rises above hydrostatic pressure, it signalizes a layer with fine particle content (clay, silt, silty sand) and contractive behavior. Soils which perform dilatant behavior show very low or negative pore pressure values. This is typical for overconsolidated clays, dense fine sands, dense silty sands and dilatative silts.

Data interpretation based on qt, Fs and u2 developments is presented in Figure 20. As can be seen, the profile can be divided into two main layers – sand and clay. Sand layer is characterized by low friction ratio *Rf*, high corrected tip resistance *qt* and pore pressure roughly equal to hydrostatic pore pressure. From the depth of 7.5 meters, the trend rapidly changes and begins to have a character of clay soil type, i.e. higher friction ratio *Rf*, low tip resistance *qt* and high positive pore pressure u_2. This general development can be seen in all preformed CPTU (Figure B1.3 and B1.4).

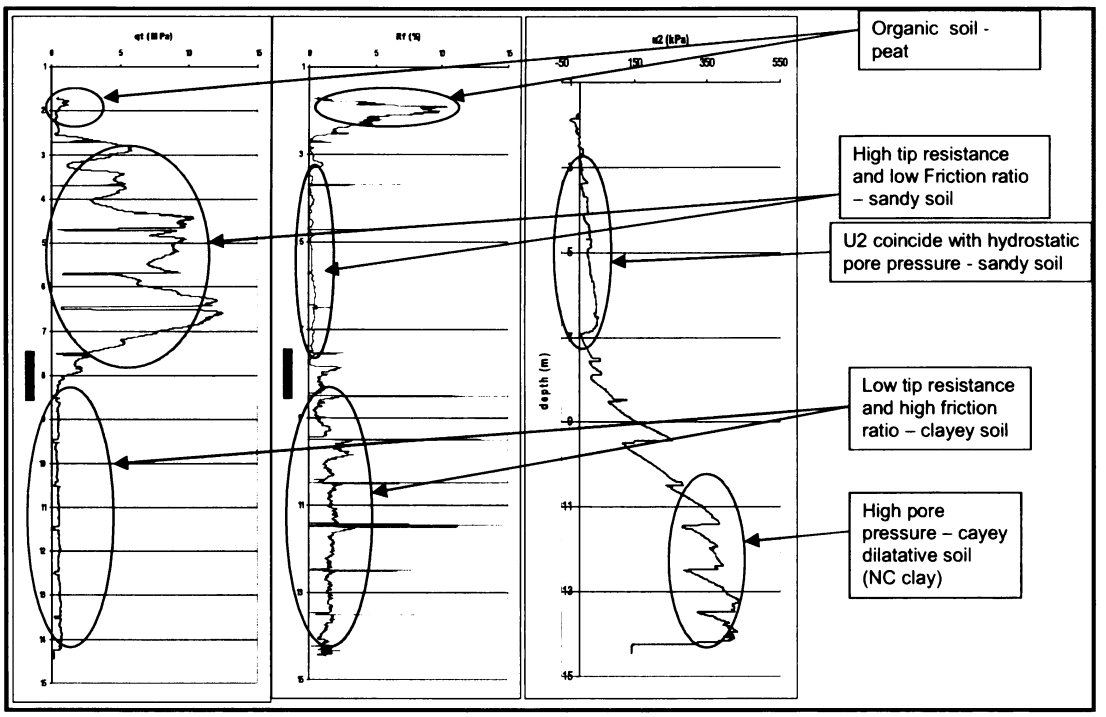

Figure 20: Readings from piezocone test BP1/2 and their interpretation. The same trend can be observed for the tests BP3 and BP4 (Figures B1.3 and B1.4)

2.2 Dissipation test

The permeability of soil, therefore its drainage properties, are an important clue to a soil profile and soil type determination. The water level at Belle Plaine site was detected at depth 0.7m.
Four sensors (Figure 19) were installed on the site, each measuring dissipation at different position. The readings were plotted into dissipation charts (time versus u_2) which are shown in Figure B2.2. The resulting pore pressures at t_{100} were plotted versus the depth and it was proved, that they coincide with the hydrostatic pressure (Figure B2.1). This certifies the reliability of the sensor measurements.

Based on dissipation curves, t_{50} was evaluated resulting in following values:

Depth [m]	Sensor1	Sensor2	Sensor3	Sensor4
3.3	1.2 min			
3.35		1.3 min		
4			0.35 min	
4.35		0.4 min		
4.7		0.3 min		

5			0.25 min	
5.7			0.3 min	
5.9				0.28 min(?)
6.7				0.16 min
6.9				0.22 min(?)
7.1				0.7 min

Table 5: t50 measured by different sensors at different depths

According to chart published by Parez and Fauriel (1988) and shown in Figure 21, the soil can be classified according to its t_{50} (Table 5). Using this chart, the values of t_{50} for soil from 4m to 6.9m are values typical for silty sand to sandy silt. High t_{50} for depths 3.3m, 3.35m and 7.1m is characteristic for silt.

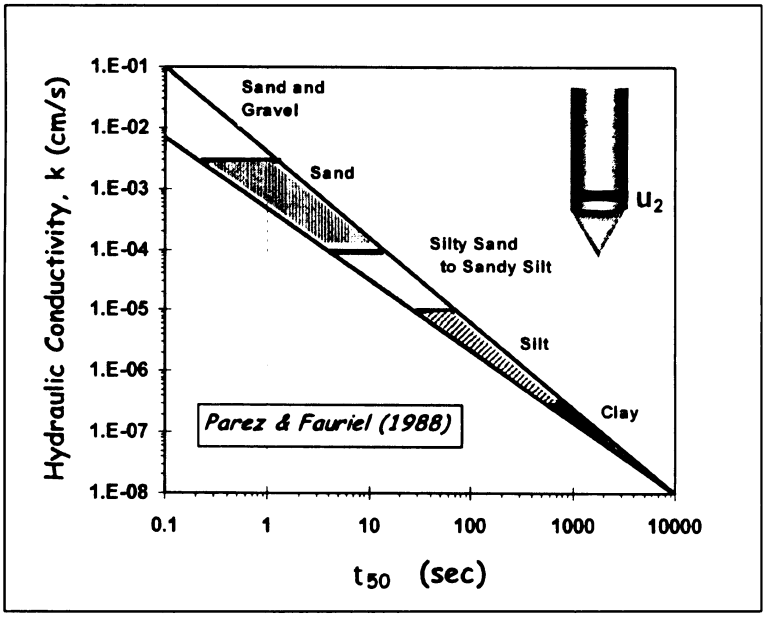

Figure 21: Chart after Parez and Fauriel (1988) classifying the soil according to t50

2.3 Classification charts

To classify a soil type, numerous *soil classification charts* were developed. These charts differ as knowledge about CPTU was improved and as different authors tried to consider different

combination of measured parameters. In early stages, only tip resistance and sleeve friction were considered in the classification charts (for review see Lunne et al., 1997). Practice showed that pore pressure measurements were found to be more reliable than sleeve friction values and so in 1984, Janbu and Senneset developed a chart classifying soil type according to its pore pressure parameter *Bq* and corrected tip resistance *qt*. Two years later, Robertson et al. made an attempt to combine all three measured parameters (*qc*, u_2, *fs*) and developed a classification comparing not only *Bq* versus corrected cone resistance *qt*, but also Friction ratio *Rf* versus *qt* (for review see Lunne et al.,1997). These charts can be viewed in Appenix B.

The values of *qc*, u_2 and *fs* increase with depth. Because previously mentioned charts don't assume the effects of overburden stress, they should not be used for depths grater than 30m. In 1990, Robertson developed a chart based on the normalized values, i.e. *Qt*, *Fr* and *Bq*. This chart is now widely used in practice and is shown in Figure 22 (for review see Lunne et al., 1997).

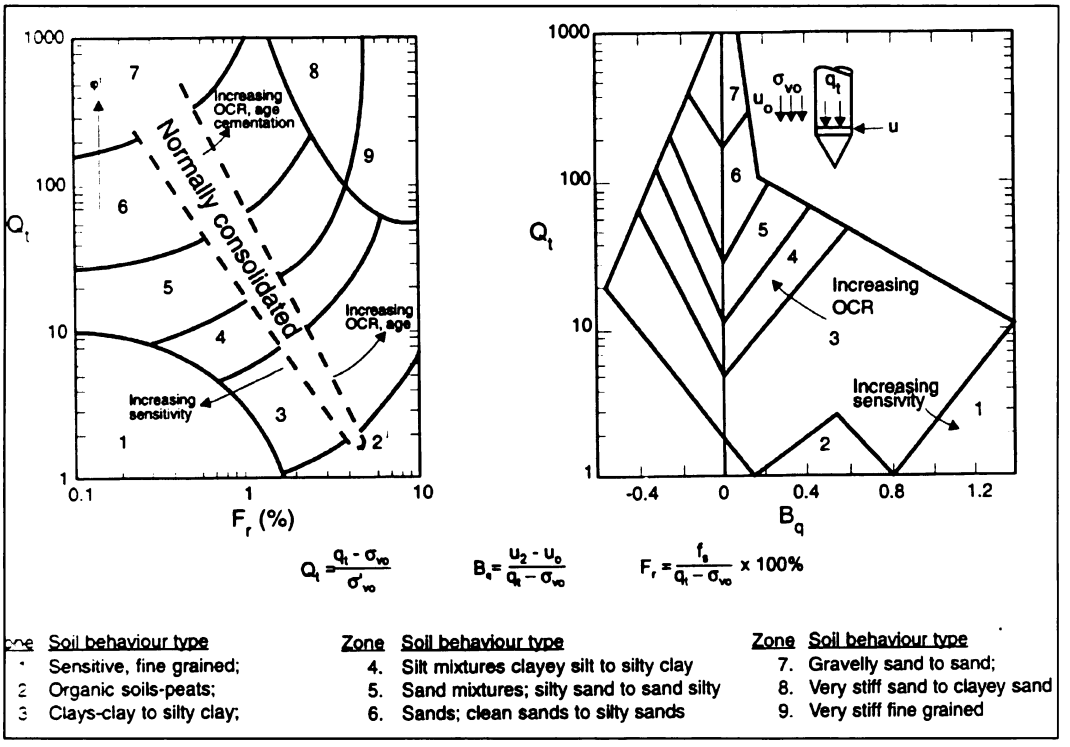

Figure 22: Soil type classification chart (for review see Lunne et al., 1997)

In order to interpret measured data from piezocone tests, the profile was divided into 0.5m layers, which were plotted into the classification charts. According to the results and considering results from other classification procedures, the profile was subdivided into the following layers:

- Gravel
- Peat
- Transition zone I
- Sand
- Transition zone II
- Clay

Graph plotting CPTU readings for these layers can be seen in Figure 23. When comparing with classification chart published by Robertson (1990) in Figure 22, it can be seen that the results confirm the chosen stratigraphical division. Application of other previously mentioned classification charts to our profile is shown in Appendix B. The obtained results are in agreement.

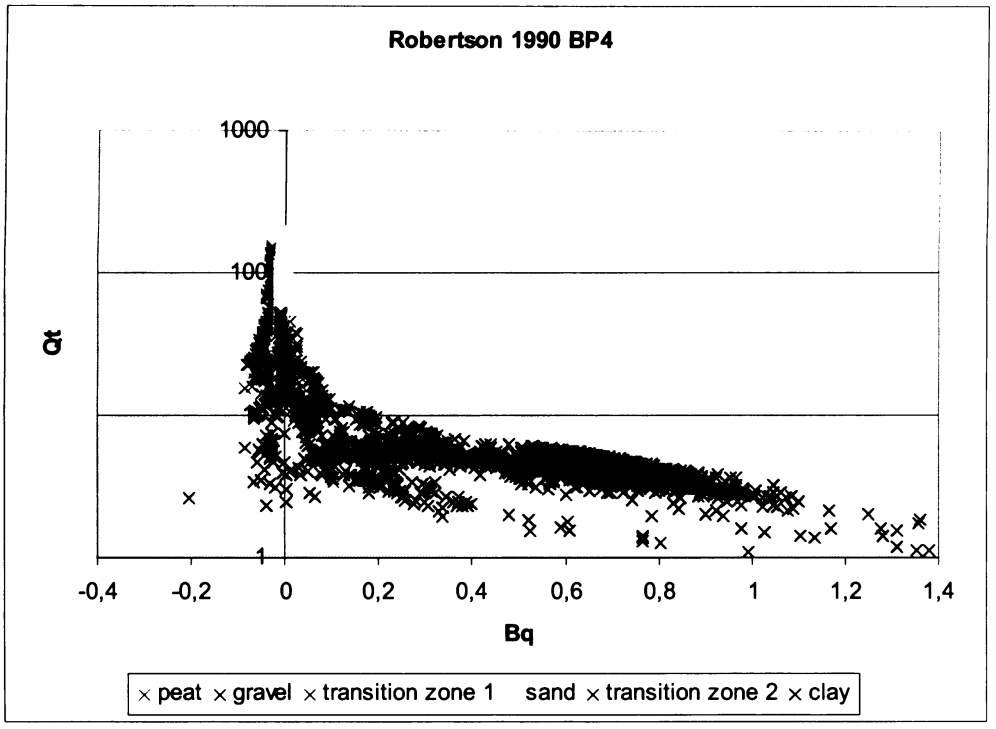

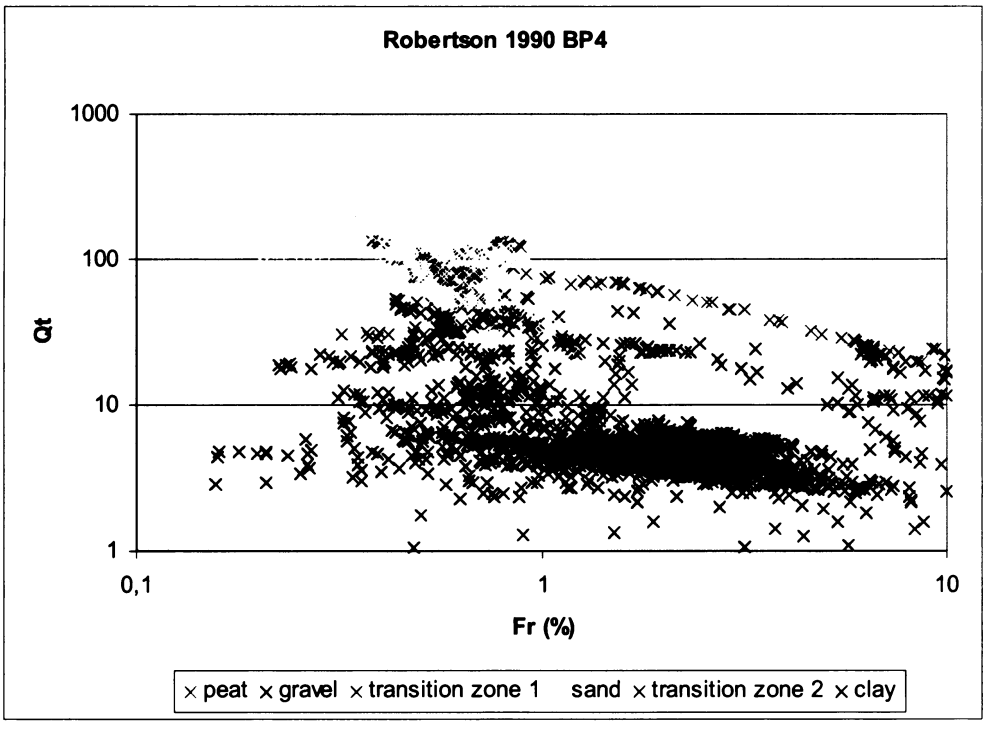

Figure 23: Soil behaviour classification applied to CPTU data from Belle Plaine

2.4 Conclusion

Based on general interpretation of our data, classification charts and dissipation tests, soil profile was divided into 6 different layers:

0m - 1.9m:

The top horizon was formed by an artificial layer of *gravel/fill*. As noted by people present during the CPTU, the fill was very compacted with high strength properties.

1.9m – 2.5m:

Based on low *qc* and extremely high friction ratio observed in CPT readings, this layer was evaluated as a *peat* layer.

2.5m - 3.5m:

The character of this layer was not clearly defined, although this could be expected, as this zone is a transition between the peat horizon and the sand underlayer. Relatively low permeability shown in the dissipation tests is probably induced by silty character of the layer. In following text, this layer will be referred to as *Transition zone I.*

3.5m - 7.5m:

Based on the classification methods listed previously, this layer was defined to be *sand* layer. From *in-situ* investigation, this sand was claimed to be very fine. The fact that t_{50} is quite high for a sand layer is assumed to be caused by the very fine character of the sand.

7.5m - 8.5m:

This layer forms a transition between the sand and clay horizon. The interpretation of the soil type is again very limited, the same as in case of Transition zone I. This zone will further on be referred to as *Transition zone II* and it is assumed to have sandy character in its upper part and clayey character in its lower part.

8.5m - 14.6m:

Using the listed classification methods, this layer was defined as a *clay* layer with possible presence of clay lenses of sensitive nature. Unfortunately the permeability of this layer is not known, because the last performed dissipation test was at depth 7.1m. Although, because of the continuous pore pressure readings, pore pressure was monitored also in the "unloading stages" when the rods were added. Having these pore

pressure readings and knowing, that adding of a rod takes approximately five minutes, very rough permeability estimation can be done. When looking at pore pressure register for BP4 (Figure B1.4), it can be seen that the pore pressure was very far from reaching the hydrostatic pressure even in the five minutes that were needed for the rod addition. This shows a very low permeability, which is characteristic for clay.

14.55m - 14.75m:

The CPT for BP4 was done into grater depths then for BP1/2 and BP3. Thanks to this, it was possible to register a thin layer with abnormal behavior. This layer is characterized by high *qc* and by pore pressure values very similar to values of hydrostatic water pressure. Based on these *qc* and u_2 readings, the layer was evaluated as thin *sand* layer.

14.75m – 30m

The thin sand layer forms only a lens in the clay horizon. From the depth of 14.75m, clay forms the profile again and is assumed to continue until the bedrock is reached.

3 Soil Characteristics

3.1 Sand layer (3.5m to 7.5m)

Cone resistance in sand is controlled not only by applied effective stress, but also by relative density of sand layer (Figure C1.1.) and sand compressibility (for review see Lunne et al., 1997).

Compressibility of sand is influenced by:

- grading of sand (uniformly graded sand is generally more compressible)
- angularity of grains (compressibility increases with angularity)
- mica and feldspar content (rising mica and feldspar content increase the compressibility)

(for review see Lunne at al., 1997)

Relative density:

ed on extensive work in large calibration chambers. Unfortunately the trend in data obtained from CPT is not so clear. A suggestion of an approximation curve is shown in Figure C1.2. This would indicate relative density over 80

Figure C1.1. is bas%.

Small Strain shear modulus (*Go*):

Maximal value of shear modulus corresponds to very low strain and decreases with growing strain. Following correlation is based on elastic theory and gives a relation between soil density ρ, shear wave velocity *Vs* and shear modulus *Go* (for review see Lunne et al., 1997):

$$Go = \rho\, Vs^2 \qquad (8)$$

When no seismic measurements available, *Go* can be evaluated empirically, although it has to be noted, that obtained results can be less reliable. The following relation was developed by Rix and Stokoe (1992) (for review see Lunne et al., 1997):

$$(Go/qc)_{ave} = 1634\ (qc/\sqrt{\sigma'_{vo}})^{-0.75} \qquad (9)$$

Using the above formulations, the value of shear wave velocity for sand was evaluated between 150m/s and 200m/s. Comparing this value with the results by Ghionna and Jamiolkowski (1995) for

river sand, 150-200m/s would correspond to shear wave velocity in river sand for lower depths, i.e. depths up to 8m.

3.2 Clay layer (8.5m to 14.5m)

Overconsolidation Ratio (*OCR*):

OCR is a ratio of highest stress that the soil experienced and the current stress. That means that the higher OCR, the higher the stress experienced by the soil[20]. If OCR is one, it means that the soil is normally consolidated (i.e. the soil is currently experiencing the highest stress in its history).

There are ways to estimate OCR from CPT and CPTU data. It is suggested that following equation should be valid for normally consolidated soil (for review see Lunne et al., 1997):

$$Qt = qt - \sigma_{vo} / \sigma'_{vo} = 2.5 \text{ to } 5 \qquad (10)$$

According to this correlation, the fine soil from 8.5m to 14.45m is normally consolidated, possibly slightly overconsolidated in the upper parts of the clay horizon.

Small Strain shear modulus (*Go*):

Shear wave velocity can be either measured by seismic methods or can be estimated empirically. Empirical evaluation of shear wave velocity is of course less reliable then in situ measurements, but can also be used in cases when no seismic readings are available.

Relation between small shear strain modulus *Go*, void ratio *e* and corrected cone penetration resistance *qt* was proposed by Mayne and Rix (1993) (for review see Lunne et al., 1997) and is described by the following equation:

$$Go = 99.5\ (pa)^{0.305}\ (qt)^{0.695}/(eo)^{1.130} \qquad (11)$$

where *pa* is reference stress – atmospheric pressure 1 atm [21]

[20] If soil is aged or cemented, the obtained OCR ratio can be misleading

[21] pressure 1 atm. = 101.325kPa

Using the results of laboratory tests done by LMSS-Mat, the value of void ratio for our clay was averaged to 1.1. Subsequently a calculation of Go and Vs could be done according to equation *(11)*, resulting in shear wave velocity between 100m/s and 150m/s.

4 Liquefaction potential of Belle Paine site

Fill/Gravel (0m-1.9m)

To initiate liquefaction, soil has to be saturated with water. On the site, water level was found 0.7 meters below the ground surface.

Generally, fill is not susceptible to liquefaction, because it is too permeable to generate high pore pressures needed for the liquefaction initiation. An exception would be, if fill was surrounded by impermeable layers. In this case, liquefaction could occur. For the case studied, no impermeable layers were found in the upper part of the profile.

Based on the above mentioned information, the fill layer is believed to be *non-susceptible to liquefaction.*

Peat (1.9m-2.5m)

Neither Robertson method nor Seed method could be used to compute the FS of peat horizon. This is because peat gives Ic higher than 2.6, therefore FS cannot be evaluated by Robertson. As for Seed method, there are no evaluation curves that can be applied for peat. In general, peat is believed to be *potentially non-liquefiable.*

Transition zone I (2.5m-3.5m)

This zone forms an underlayer to the peat horizon and is supposed to be very sandy with characteristics similar to the clear sand horizon. Seed and Robertson analysis show that there is a less liquefiable layer within the transition zone, although it can't be designated as non-susceptible to liquefaction.

Transition Zone 1 is claimed to be *potentially liquefiable.* This is based on the following:

- Robertson and Seed analysis result in FS lower than 1
- Graphical evaluation according to Robertson chart shows that Transition zone 1 is situated in the A zone of the chart, that means in a zone where soil is potentially liquefiable.
- Sandy character of the layer
- Saturation by water
- Low compaction given by young age of the sediment

Sand (3.5m-7.5m)

The position of the site and vegetation found in its surroundings can give information about the soil profile and soil characteristics. The site of interest is found in costal area, which is a depositional environment formed by relatively young sediments. Close to the site is mangrove vegetation, which requires specific conditions for its growth. The soil profile in mangrove areas is saturated and usually consists of bottom clay layer, middle sand layer and top mud horizon. Sediments in costal areas are usually aeolian or fluvial deposits. These sediments are uniformly graded and smoothened by water and wind transport.

Low compaction, uniform gradation and young age are factors making sand more susceptible to liquefaction.

The results of Seed and Robertson analysis for the sand layer are presented in Figure 24. Comparing the two methods, it can be seen that Robertson method gives a slightly lower factor of safety.

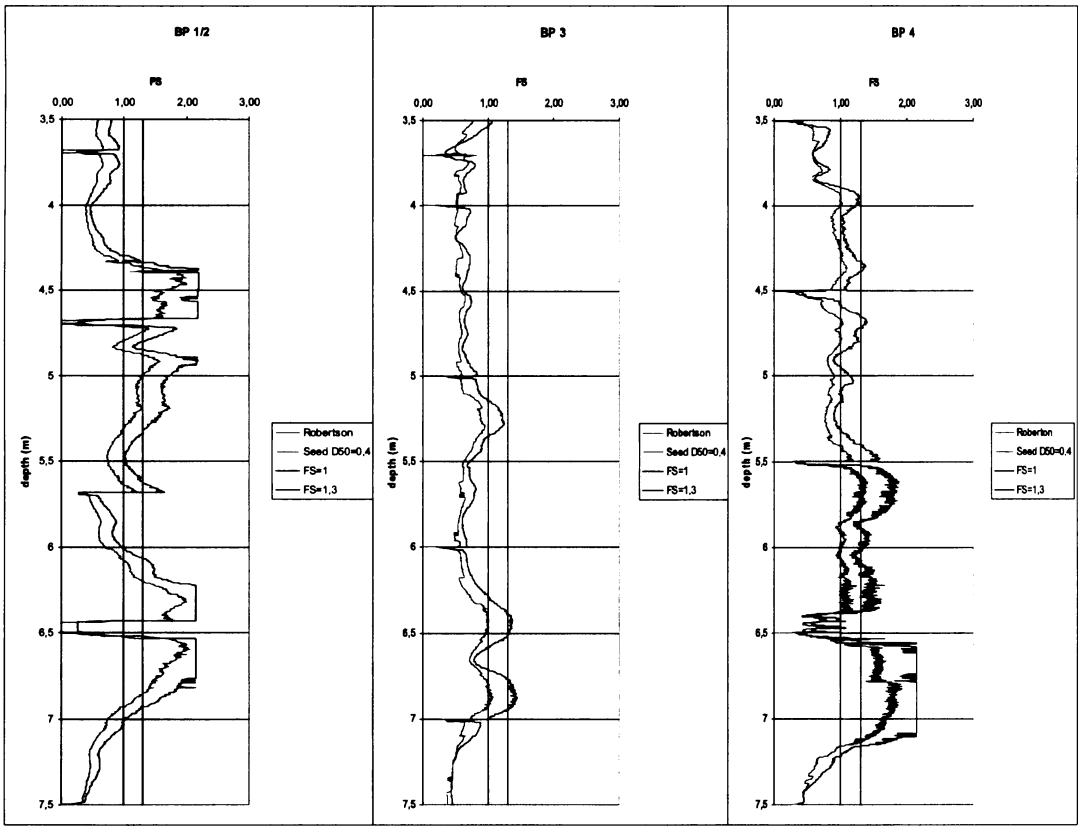

Figure 24: - Comparison of Seed and Robertson analysis for BP1/2, BP3 and BP4 (results of Seed analysis are in red; Robertson analysis in green)

Presented Seed analysis was preformed with the assumption of clean sand, even though formally four possible fine contents were considered in the analysis (≥35%; ≈15%; ≈10%; ≤5%; respectively D_{50}=0.1mm; D_{50}=0.2mm; D_{50}=0.25mm; D_{50}=0.4mm). Granulometric analysis done by CERMES showed following D_{50} for samples at different depths of the sand horizon:

4m – 5m: D_{50} = 0.05 mm

4.7m – 5.5m: D_{50} = 0.16 mm

5.5m – 6.5m: D_{50} = 0.14 mm

This would suggest using values of FS given for curves FC≥35% to FC≈15%. Despite this fact, the assumption of clean sand was chosen to be more correct thanks to the following:

- Curves given by Seed relate D_{50} of soil with silty or clayey particles. *In situ* evaluation of borings in the analyzed depths claimed clean but very fine sand with low D_{50}. For the absence of silty or clayey particles, a curve for clean sand was used.
- Comparing Robertson analysis with Seed analyses for different fine content, FS given by Robertson is closest to FS given by Seed for clean sand. Because Robertson analysis incorporates the calculation of fine content, it should give values of FS already adjusted to the influence of fine content.
- Selection of a curve for no fine content is most conservative, as according to Seed (Figure 10), the factor of safety increases with growing percentage of fine content. This fact will be further discussed.

Figure 24 can be summarized into the following:.

- In depth 4.5m-5.5m seem to exist less-liquefable to non-liquifable soil lenses.
- Not susceptible to liquefaction are assumed to be two lenses situated somewhere in depth form 6m to7.5m.
- The rest of the profile can be considered as liquefiable

Based on Robertson and Seed analysis, the sand horizon in general would be described as *potentially liquefiable*. This was confirmed by both graphical methods (Robertson chart and graph Bq versus qt) where the sand layer was plotted into the critical zones (Appendix D).

Transition zone II (7.5-8.5):

This zone is a transition between the clay and sand layer. The upper part of the layer has still sandy character; lower part has probably more silty to clayey character. Based on FS given by

Robertson and Seed, the upper part of the layer (i.e. 7.5m-8m) is assumed to be *potentially liquefiable.* For the lower part of this transition zone, Roberson analysis could not be used, because Ic was evaluated as higher than 2.6. Also Seed method was found to be inappropriate, because the values of qc1 were too low to be able to plot the critical cyclic stress ratio. For the high percentage of fine content in the lower part of Transition zone II, this part was assumed to be *potentially non-liquefiable.*

Using graphical evaluation Bq versus qt , the Transition zone II is almost entirely plotted into non-liquefiable area. Robertson graphical evaluation was not used, because the Transition zone 2 is plotted in a way that it belongs to all three zones (A,B,C).

Clay (8.5m-14.5m):

Clay in our profile could not be analyzed for liquefaction by Seed analysis. This was because qc1 was very low, fine content very high and therefore values of stress ratio couldn't be plotted. In case of Robertson analysis, Ic was evaluated as higher than 2.6. In this case, it is suggested to use other evaluating criteria but it is also said, that if the normalized friction ratio *Fr* is grater than 1%, the soil is likely to be non-liquefiable. It was proved that *Fr* is grater than 1 for almost entire clay profile.

Using the graphical methods, it can be seen that on *Bq* versus *qt* chart, the entire clay layer is in non-liquefaible zone. In the Robertson chart, most of the clay layer is plotted into zone B, which means non-liquefiable although it suggests that there can be small amount of sensitive clay, which can be potentially liquefiable.

This layer was evaluated as *potentially non-liquefiable.* The possibility of liquefaction of sensitive clay lenses can not be excluded nevertheless is claimed to be unlike.

5 Concluding remarks

The aim of the previous chapters was to interpret soil profile at Belle Plaine site and evaluate the liquefaction potential of stratigraphical layers. The soil profile interpretation was done according to the Figure 25., i.e. fill (0m-1.9m); peat (1.9m-2.5m); sand (3.5m-7.5m) and clay (8.5m-bedrock). Horizons forming a boundary between two soil types are difficult to classify. In order to separate these zones with the uncertain soil classification, the transition zone I and II were defined. Transition zone I forms a boundary between peat and sand; Transition zone II divides the sand horizon from clay horizon.

The soil profile interpreted from the CPTU data does not coincide with the geological *in-situ* evaluation of the borings, which was done by *ANTEA, Ingéniérie et conseil.* These borings – SC1 and SC2 – are marked on a situation layout shown in Figure A1.2. The results of site evaluation of SC-1 and SC-2 define sand horizon until 9.5m; clayey sand from 9.5m to 11.5m and clay with variable composition from 11.5m. This interpretation is in a strong disagreement with an interpretation

proposed by this report. It is my opinion, that the radical drop in *qc* (Figure 25) has to be caused by a change in soil type, more specifically change from sandy to clayey soil type.

Figure 24 shows an interpretation and evaluation of BP1/2 readings and was chosen to represent the results for the whole site. This was done because the readings for BP1/2 weren't adjusted as was done for readings for BP3 and BP4. Friction ratio registered during the penetration BP3 and BP4 was negative, which was probably caused by wrong calibration or shift of the sleeve friction data (negative values of friction in soil are not possible). After an experienced judgment, the values of sleeve friction ratio were increased by 9kPa for BP3 and 12kPa for BP4. Nevertheless, readings for BP1/2 are assumed to be most reliable.

The liquefaction potential was evaluated by Seed and Robertson empirical methods and by Robertson and Bq versus qt graphical methods. Seed and Robertson methods incorporate evaluation of cyclic stress ratio induced by an earthquake. This is done according to equations *(1)*, *(2)* and *(4)*. As can be seen from these equations, parameter of peak horizontal acceleration (a_{max}) is in a direct proportion to the resulting cyclic stress. For the case of Belle Plaine site, a_{max} was set to a value 0.2g. This value is based on seismic hazard maps[22].

Combining the results of Seed and Robertson empirical method and Robertson and Bq versus qt graphical methods, Transition zone I, Sand horizon and the upper part of Transition zone II were evaluated as potentially liquefiable. This makes the soil profile at Belle Plaine potentially liquefiable from the depth of 2.5 meters to 8 meters. In this section of the profile are soil lenses with higher factor of safety; the most dominant are lenses at depths 6m-7.5m, which were registered in all CPT readings.

Seed method proposes evaluation of cyclic stress ratio based on values of *qc* (for CPT) and fine content. As can be seen form Figure 10, the most conservative results are obtained while assuming zero fine content. As later researches claim, ignoring the presence of fines in order to get most conservative result is a mistake. Fines can either decrease the cyclic stress ratio or increase and which, depends on many factors. It was said by Troncoso (1990) in Prakash and Puri, (2003) that factor of safety for sands decreases with fine content up to 20-30% of the soil's weight. At this stage, the sand has minimum cyclic stress ratio, therefore has the highest potential to liquefy. After reaching the value of 20%, the cyclic resistance of sand starts to increase with the growing fine content.

[22] Seismic hazard maps are maps determining most common peak horizontal acceleration for a particular area

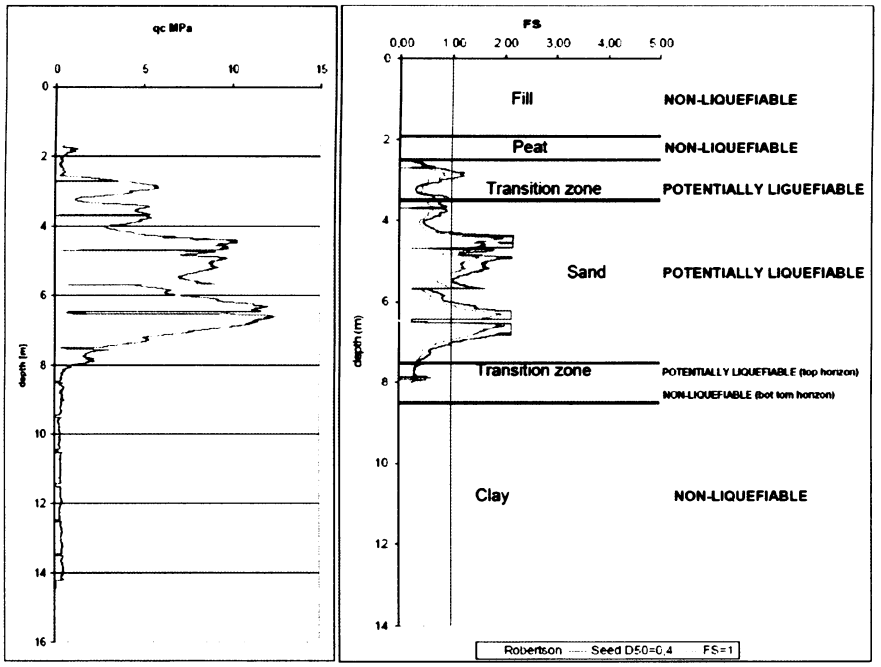

Figure 25: Evaluation of soil profile and liquefaction potential (on the right); qc development (on the left)

Sand horizon is assumed to be composed of clean fine sand and so the evaluated results of factor of safety are claimed to be reliable. Although as previously mentioned, the transition zones are very difficult to classify for their soil type and so the evaluation by Seed method assuming zero fine content can be misleading.

Clay content generally increases the cyclic stress ratio, therefore increases the factor of safety. Zhou (1987) (for reference see Prakash and Puri, 2003) made an observation that after reaching a certain percentage of clay content in soil, the soil won't liquefy. He related this clay content to earthquake intensity:

Intensity	7	8	9
Clay content	10%	13%	16%

From the CPTU interpretation, clay forms the profile from the depth of approximately 8.5 metres. Referring to previously mentioned, this clay was said to be non-susceptible to liquefaction.

The evaluation of liquefaction potential was done considering an earthquake acceleration of 0.2m/s and earthquake magnitude of 7.5. If higher values were considered, the factor of safety would decrease.

Liquefaction of sands has been extensively studied. Unfortunately the natural conditions are usually not so favorable and more complicated soil types have to be analyzed.

The evaluation for silty sands, silts and silt-clay mixtures is still a challenge; the effect of fine content in sand is still being investigated. Considering the consequences of liquefying soils in urban areas, it is my opinion that there is a need to clarify the subject of soil liquefaction and propose other reliable evaluation method.

PART IV – NUMERICAL SIMPLIFIED MODELING OF SEIMIC *BELLE PLAINE* SITE RESPONSE

1 Introduction

The aim of this section is to simulate earthquake conditions at Belle Plaine site and compare results that were obtained empirically in the previous section of the report with results given by a computer code. For this purpose, PLAXIS Dynamic (2D; Version 8) was used.

PLAXIS is a two-dimensional finite element code used for geotechnical practise. With the help of various constitutive models, it predicts soil, rock and structure response in static and dynamic conditions. PLAXIS Dynamic is able to simulate vibrations, as for example earthquake cyclic loading, and model the material behaviour.

The empirical analyses preformed in the first part of this report were done according to Seed and Robertson method. Both of these methods characterize the earthquake loading by a simplified approach after Seed and Idriss (1971), i.e.

$$\tau_{cyc} = 0.65\, a_{max}/g\, \sigma_v\, r_d \qquad (12)$$

where a_{max} is the peak horizontal acceleration, σ_v is the total vertical stress and *rd* is a stress reduction factor. τ_{cyc} represents shear stress with uniform amplitude. This amplitude is equal to $0.65\tau_{max}$ where τ_{max} is the maximum shear stress induced by the earthquake. Seed also defined the number of uniform shear stress cycles needed to produce pore pressures equivalent to pore pressures induced by an earthquake with irregular time history.

This approach assumes that the induced cyclic shear stresses characterize development of excess pore pressures and therefore can be used to evaluate the liquefaction potential.

2 Input

PLAXIS Dynamic was used for numerical computation of shear stresses induced at Belle Plaine site. An earthquake with maximal horizontal acceleration 0.24g was imposed at the depth of 30 meters, i.e. at the bedrock level. To simulate real conditions, accelerogram from an earthquake registered in California in year 1989 was used. A 2D plane strain model with 15-node elements was

applied to the Belle Plaine profile, where the geometry was divided into four layers of different thickness:

LAYER	DEPTH
Gravel	0m-2m
Peat	2m-3m
Sand	3m-8m
Clay	8m-30m

The following parameters were introduced into the calculation:

	Clay	**Sand**	**Gravel**	**Peat**
Material Model	Mohr-Coulomb	Mohr-Coulomb	Mohr-Coulomb	Mohr-Coulomb
Material Type	Undrained	Undrained	Undrained	Undrained
Unit weight-unsaturated [kN/m^3]	15	18	20	8
Unit Weight-saturated [kN/m^3]	18	20	22	12
Eref [kN/m^2]	70 000	175 000	200 000	1 000
Poisson's Ratio	0.33	0.33	0.35	0.35
Cohesion [kN/m^2]	5.5	0	1	5
Friction Angle[°]	24	31	33	20
Dilatancy Angle [°]	0	1	3	0
Secondary wave velocity [m/s]	131.1	189.3	194.1	21.3
Primary wave velocity [m/s]	260.3	375.7	363.2	44.34

Table 6: Material parameters used in Plaxis Dynamic

Mohr-Coulomb model is a basic model used for an approximation of soil behavior. It performs linear-elastic-perfectly-plastic behavior and requires five input parameters:

- Young's modulus E
- Poisson's ratio ν
- Friction angle φ
- Dilatancy angle ψ
- Cohesion c

Mohr-Coulomb constitutive equation was applied in order to keep calculations simpler and therefore more transparent, but this was done at the expense of accuracy.

The water level was set to 0.7m depth. Because the loading and unloading of the soil during earthquake is very rapid, undrained behaviour was set for the whole soil profile.

3 Calculation and Output:

Calculation was preformed in dynamic conditions, i.e. with the following equation of motion (for review see Plaxis manual):

$$M\ddot{u} + C\dot{u} + Ku = F \qquad (13)$$

where M is a mass matrix, C is a damping matrix and K is a stiffness matrix. It can be seen, that the classical equation of motion for static conditions is extended for a damping matrix and mass matrix. Mass matrix introduces soil mass, water mass and construction mass into the calculation. The damping matrix introduces energy dissipation into the system. This energy dissipation is caused mainly by friction, heat generation and plastic yielding. Damping matrix can be calculated as a function of mass M and stiffness K of the system (Rayleigh damping)

$$C=\alpha M + \beta K \qquad (14)$$

where α and β are so called Rayleigh coefficients and are a function of damping ratio and frequency of vibration. Values of α and β were not introduced in the final calculation as their values didn't seem to have a big influence on the obtained results.

Plaxis Dynamic simulated cyclic loading with resulting shear stresses (Figure 28). Plotting maximal values of σ'_{xy} against depth, a comparison with empirical results obtained from Seed and Idriss (1971) equation could be made (Figure 26).

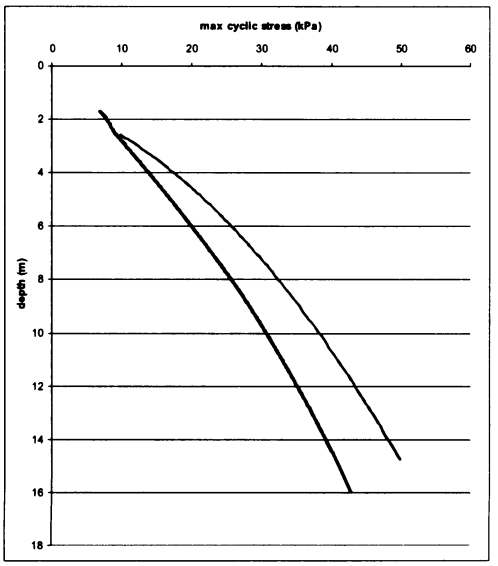

Figure 26: Maximal shear stress imposed by the earthquake versus depth; red line represents results obtained empirically, green line represent values given by numerical code PLAXIS Dynamic

4 Conclusion:

The aim of this section was to compare values of maximal cyclic shear stress predicted by numerical code with values of maximal cyclic shear stress given by the following simplified equation (after Seed and Idriss, 1971):

$$\tau_{max} = (a_{max}/g)\, \sigma_v\, r_d \qquad (2)$$

This equation is used in Seed and Robertson methods for liquefaction potential evaluation.

As can be seen from Figure 26 and 27, τ_{max} values obtained by numerical modelization in PLAXIS Dynamic are relatively in agreement with the results obtained by empirical methods.

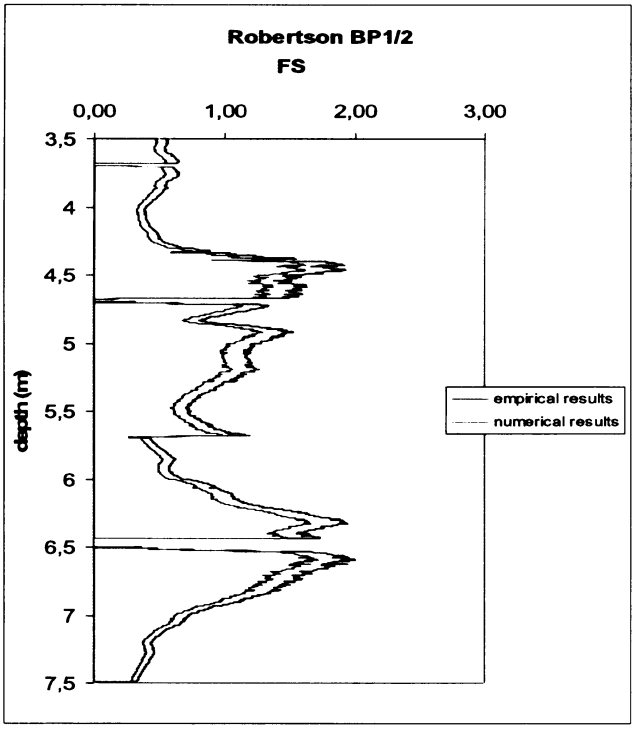

Figure 27: Comparison of FS obtained by Robertson method and FS obtained by introducing σ'xy max computed by PLAXIS Dynamic (sand layer of Belle Plaine profile)

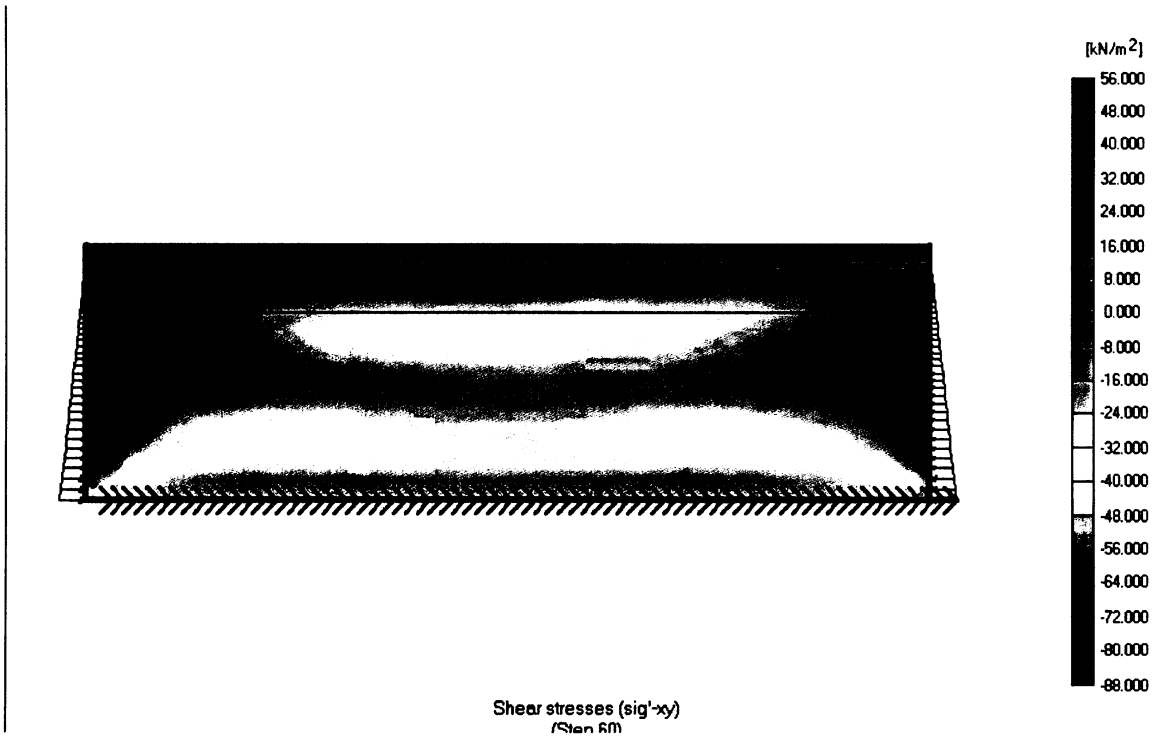

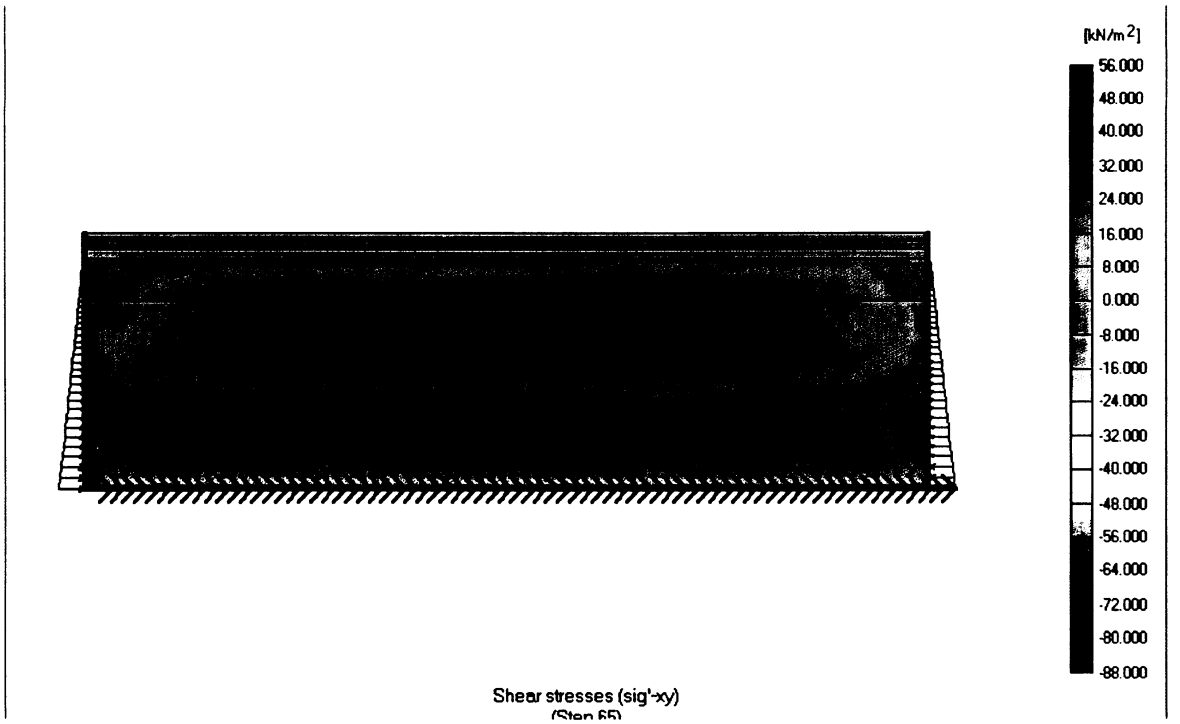

Figure 28: Cyclic shear stresses induced by earthquake, Belle Plaine

Prague, 2008

Hana Šantrůčková

.....

REFERENCES:

- ADACHI, T., IWAI, S., YASUI, M. and SATO, Y. (1992), *Settlement and inclination of reinforced concrete buildings in Dagupan City due to liquefaction during 1990 Philippine earthquake*, Proc. 10th World Conf. on Earthquake Engineering, Vol. 2

- ADALIER, K. and ELGAMAL, A. (2004), *Mitigation of liquefaction and associated ground deformations by stone columns*, Engineering Geology, 72 (2004), 275-291

- ANDRUS, R.D. and CHUNG, R.M. (1995), *Ground Improvement Techniques for Liquefaction Remediation Near existing lifelines,* on-line source: http://fire.nist.gov/bfrlpubs/build96/PDF/b96013.pdf.

- ANDRUS, R.D. and CHUNG, R.M. (1995), *Proceedings, 27th Joint Meeting of the U.S.-Japan Cooperative Program in Natural Resources Panel on Wind and Seismic Effects*, Tsukuma, Japan

- ATKINSON, J.H. (1993), *An Introduction to The Mechanics of Soils and Foundations Through Critical State Soil Mechanics*, McGraw-Hill International (UK) Limited

- BEEN, K. and JEFFRIES, M.G. (1985), *A state parameter for sands*, Géotechnique, 35, 2, 99-112

- BEEN, K., JEFFRIES, M.G. and HACHEY, J.E. (1991), *The critical state of*, Géotechnique, 41, 3, 365-381

- BHATTACHARYA, S., MADABHUSHI, S.P.G. and BOLTON, M. (2003), *Pile Instability during Earthquake Liquefaction*, ESCE Engineering Mechanics Conference (EM2003), Seattle

- BOUGUERRA, H. (1997), *Prévision du potential de liquéfaction des sites sableux l'aide d'sppareillages in-situ*, Thèse, INPG

- GHIONNA, V.N. and JAMIOLKOWSKI, M.. (1995), *Cone pressuremeter tests in Po river sand*, The Pressuremeter and its New Avenues, Ballivy (ed.)
- IDRISS, I. M. (1999), *An update of Seed-Idriss Simplified Procedure for Evaluating Liquefaction Potential*, 99th Workshop New Approaches to Liquefaction Analysis, Washington, DC

- IDRISS, I.M. and BOULANGER, R.W. (2004), *Semi-empirical procedures for evaluating liquefaction potential during earthquakes*, 11th International Conference on Soil Dynamics & Earthquake

Engineering (ICSDEE) and The 3rd International Conference on Earthquake Geotechnical engineering (ICEGE), Berkeley, California

- KRAMER, S.L. (1996), *Geotechnical Earthquake Engineering,* Prentice-Hall, Englewood Cliffs, N.J., 653

- LIU, L. and DOBRY, R. (1997), *Seismic response of shallow foundation on liquefiable sand,* Journal of Geotechnical and Geoenvironmental Engineering, June 1997.

- LUNNE, T., ROBERTSON, P.K. and POWELL, M.J.J. (1997), *Cone Penetration Testing in Geotechnical Practice,* Spon Press

- MENDOZA, M.J. (1999), *Geotechnical observations on the Tehuacan (Mexico) earthquake of June 1999*

- MIURA, S., KAWAMURA S. and YAGI, K. (1995), *Liquefaction Damage of Sandy and Volcanic Grounds in 1993 Hokkaido Nansel-Oki Earthquake*, Proc. 3rd Int. Conf. on Recent Advantages in Geotechnical Earthquake Engineering

- MOFFAT, B.S. (2008), *Soil Remediation Techniques for Reduction of Earthquake-Induced Liquefaction*, on-line source: www.succeed.ufl.edu/asce/Program/Extras%5CPres_511_662.pdf

- PAREZ, L. and FAUREIL, R. (1988). *Le piézocône. Améliorations apportées à la reconnaissance de sols,* Revue Française de Géotech, Vol. 44, 13-27

- POWELL, J.J.M.. and LUNNE, T. (2005), *Use of CPT in clays/fine grained soils*, Studia Geotechnica et Mechanica, Vol. XXVII, No. 3-4

- PRAKASH, S. and PURI, V.K. (2008), *Liquefaction of silts and silt-clay mixtures*, on-line source: http://www.ces.clemson.edu/UsTaiwanWorkshop/Paper_SDEE/SDEE_Shamsher%20Prakash.pdf.

- PURI, V.K. and PRAKASH, S. (2008), *Pile design in liquefying soil*, The 14th World Conference on Earthquake Engineering, Beijing, China

- ROBERTSON, P.K. (1990), *Soil classification using cone penetration test,*, Canadian Geotechnical Journal, 27(1): 151-158

- ROBERTSON, P.K. (1994), *Suggested terminology for liquefaction*, Proceedings of the 47th Canadian Geotechnical conference, Halifax

- ROBERTSON, P.K. and WRIDE, C.E. (1998), *Evaluating cyclic liquefaction potential using the cone penetration test*, Can. Geotech. Journal 35, pp.442-459.

- SANTRUCKOVA, H. (2007), *Liquefaction analysis for Belle Plaine site*, MSc Thesis, Laboratoire 3S-R, Grenoble

- SEED, H.B., and DE ALBA, P. (1986). *Use of SPT and CPT tests for evaluating the Liquefaction Resistance of Sands*, Proc. Conf. Use of In-Situ Tests in Geotechnical Engineering

- SEED, H.B. and IDRISS, I. M. (1971), *Simplified procedure for evaluating soil liquefaction potential*, J. Geotech. Engrg Div., ASCE, 97(9), 1249-1273

- TOKIMATSU, K., MIDORIKAWA S.,TAMURA, S., KUWAYAMA, S. and ABE, A. (1991), *Preliminary report on geotechnical aspects of the Philippine earthquake of July 16*, 1990, Proc. 2nd Int. Conf. on Recent Adv. in Geotech. Earthquake Engineering and Soil Dyn.

- WANG, W. (1979), *Some Findings in Soil Liquefaction*, Report Water Consevancy and Hydro-electric Power Scientific Research Institute, Beijing, China

- YOSHIMI, Y. and TOKIMATSU, K. (1977), *Settlement of buildings on saturated sand during earthquakes*, Soils and Foundations, 17(1).

- Zakládání Staveb (2003); Výrobní program/Production program; www.zakladani.cz; www.zakladani.com

- on-line source, unknown author: www.fugrowest.com/pdf/Ch3-Normalization.pdf

APPENDIX A

Figure A 1. 1: Belle Plaine site

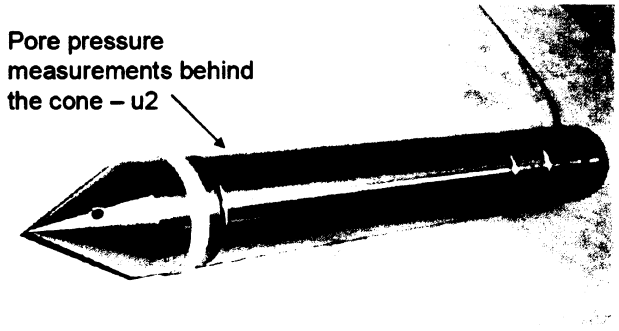

Figure A 1.3: Pore pressure measurements behind the cone

Figure A 1.2 : Situation at Belle Plaine site

APPENDIX B

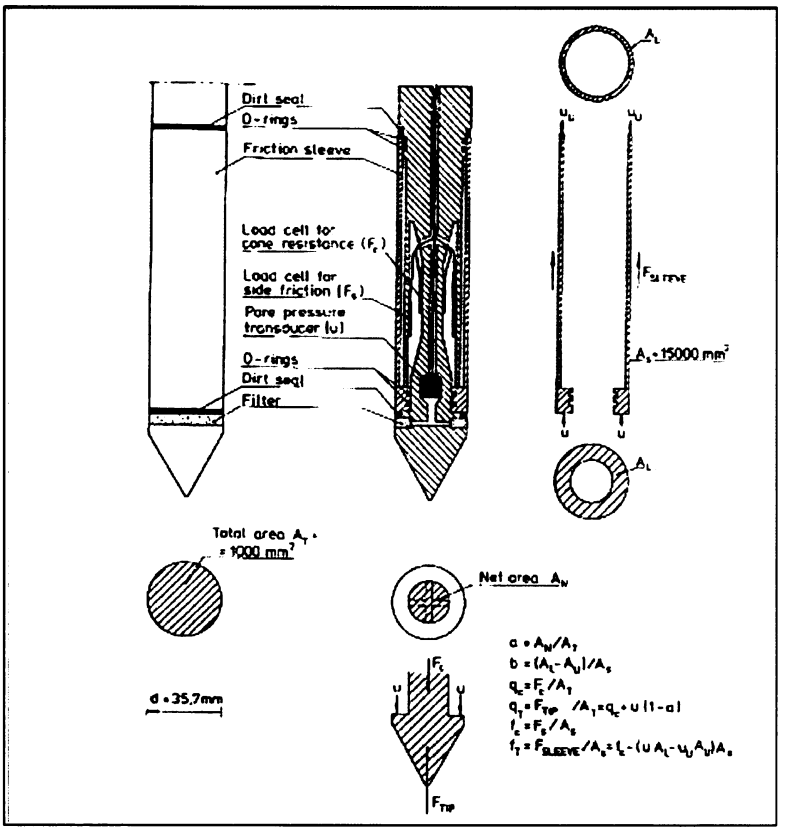

B1. 1: Design of a piezocone (for reviw see Lunne, T., Robertson, P.K. and Powell, M.J.J, 1997)

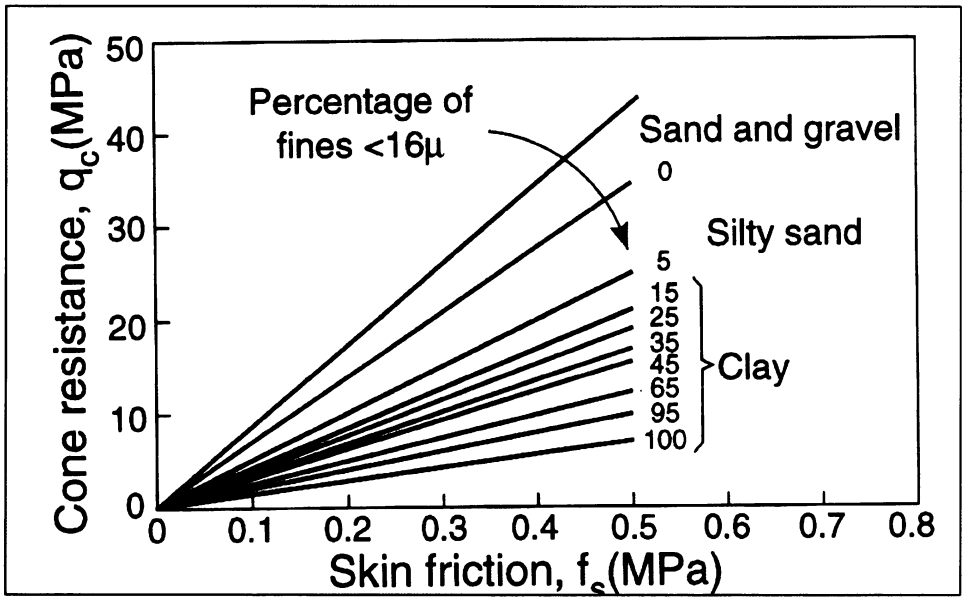

B1. 2: Relation between sleeve friction and cone resistance (from Begeman, 1965, for review see Lunne, T., Robertson, P.K. and Powell, M.J.J, 1997)

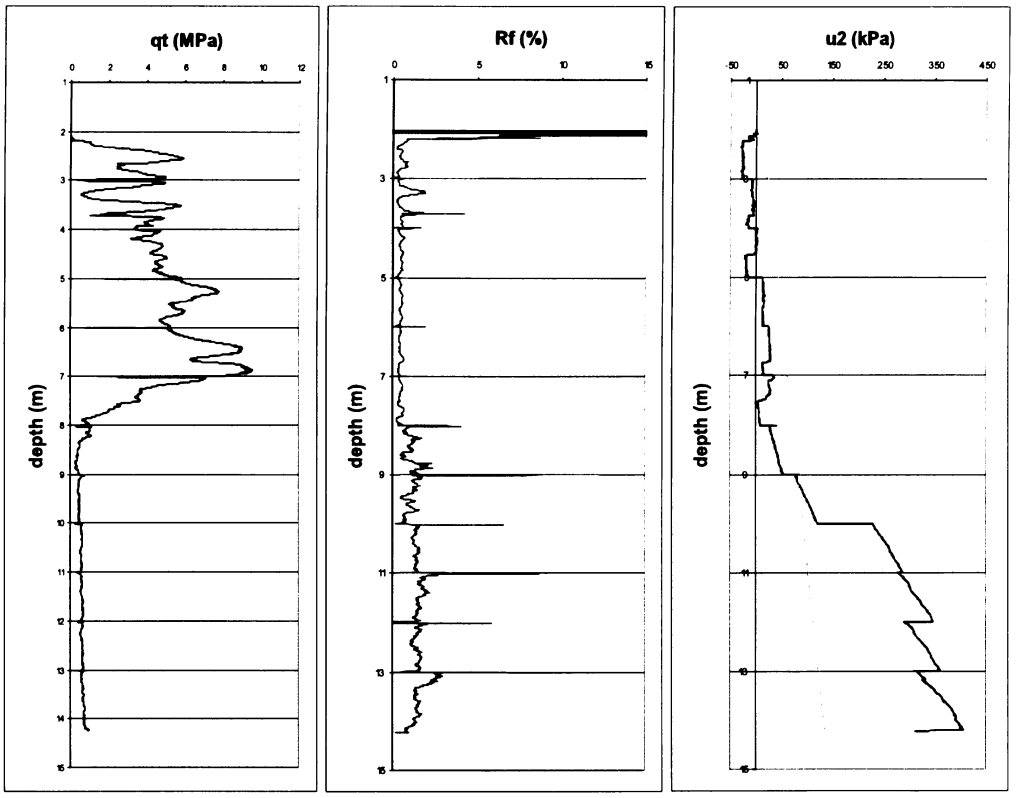

B1. 3: Readings from

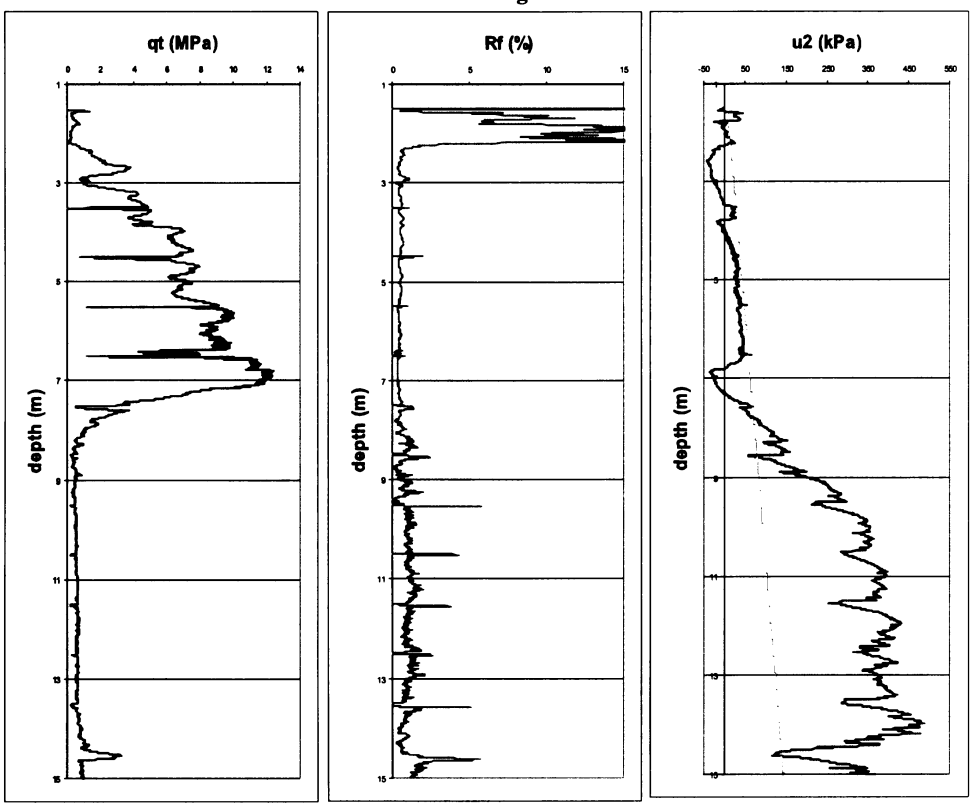

B1. 4: Readings from BP4

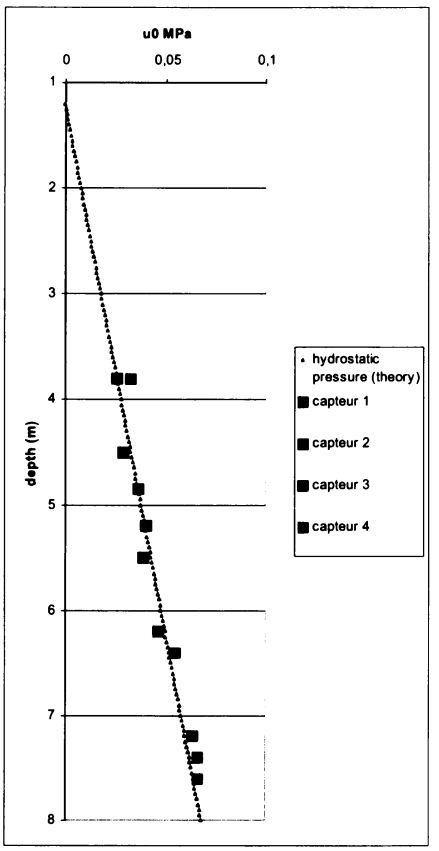

Figure B2.1: Measured t100 plotted versus depth; (dashed line represents the hydrostatic pressure)

Sensor 1 :

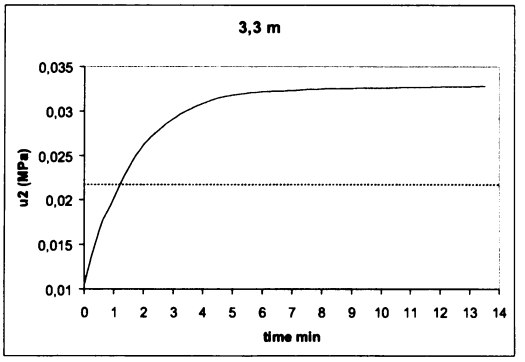

Sensor 2 :

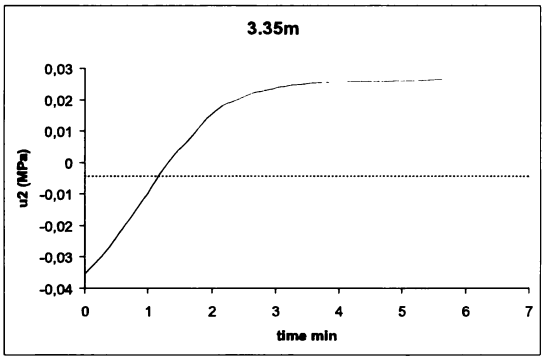

Sensor 2 :

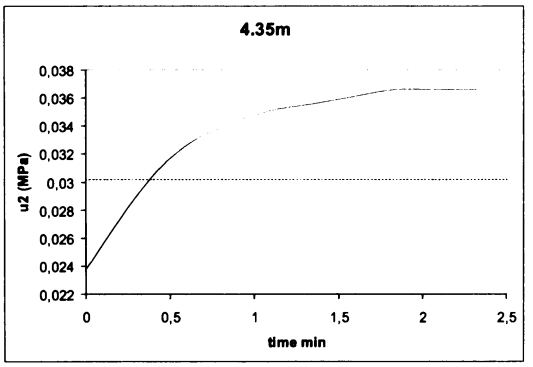

Sensor 2 :

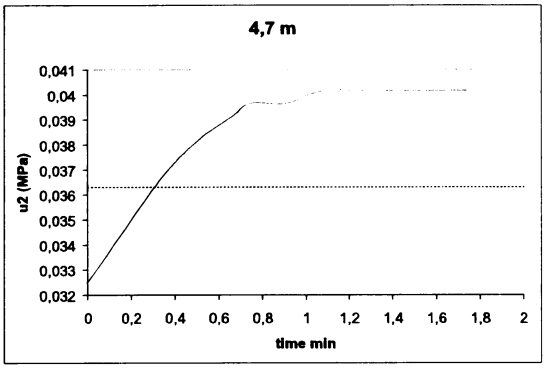

Sensor 3 :

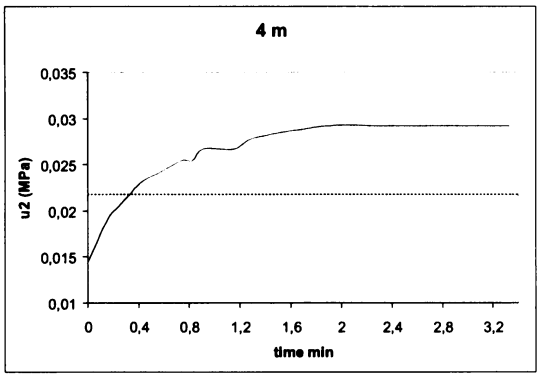

Sensor 3 :

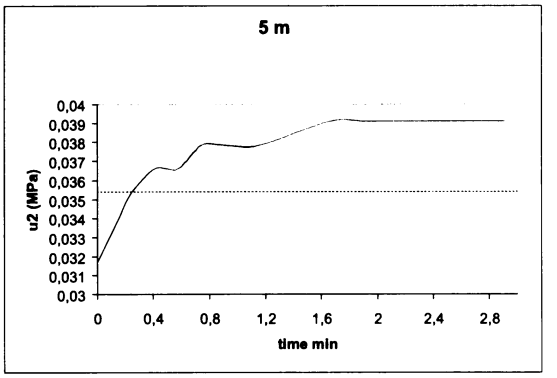

Sensor 3 :

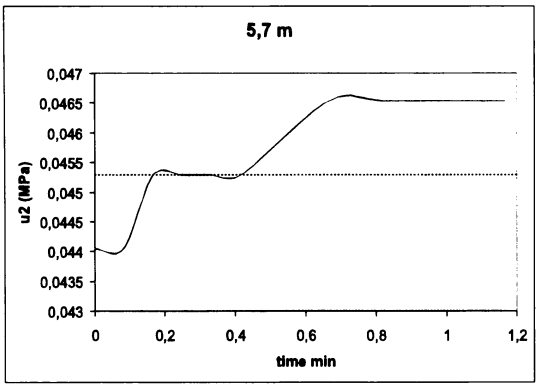

Sensor 4 :

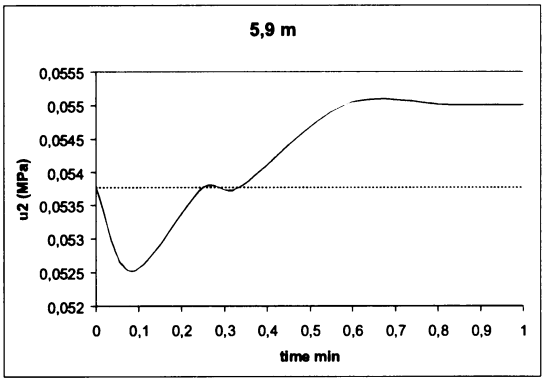

Sensor 4 :

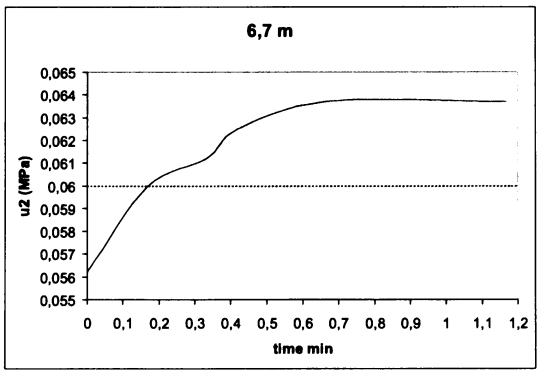

Sensor 4 :

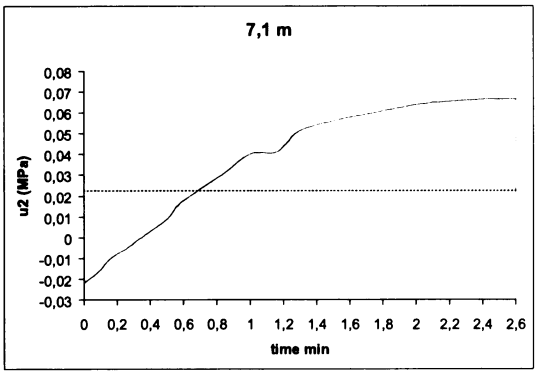

B2. 2: Dissipation charts

Classification chart after Doughlas and Olsen (1981)

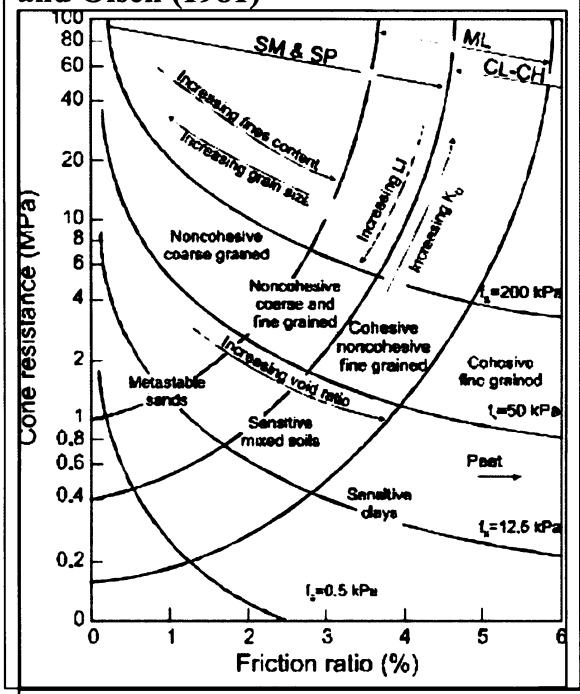

Classification chart after Janbu and Senneset (1984)

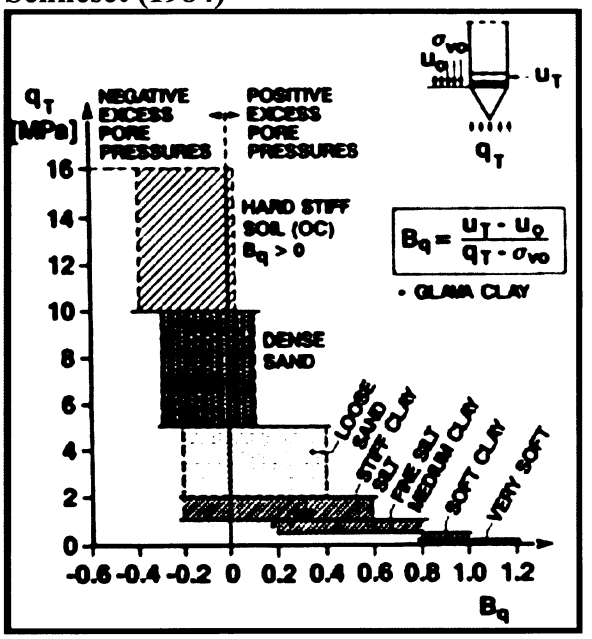

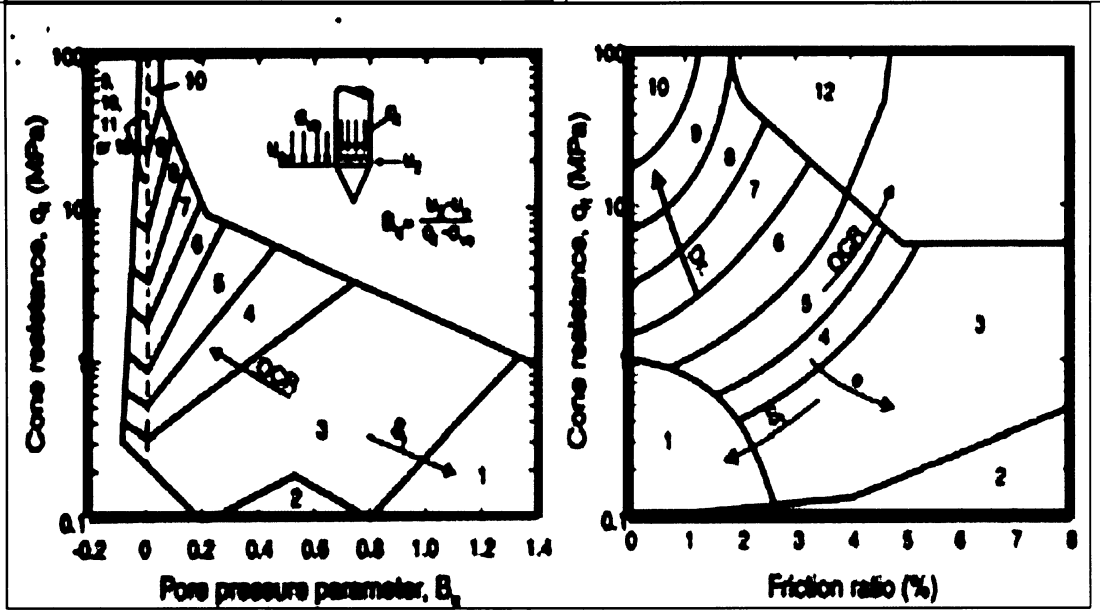

Classification chart after Robertson et al. (1986)

Zone 1. – Sensitive fine grained	Zone 4. – Silty clay to clay
Zone 2. – Organic material	Zone 5. – Clayey silt to silty clay
Zone 3. - Clay	Zone 6. – Sandy silt to clayey silt
Zone 7. – Silty sand to sandy silt	Zone 10. – Gravelly sand to sand
Zone 8. – Sand to silty sand	Zone 11. – Very stiff fine grained
Zone 9. -Sand	Zone 12 – Sand to clayey sand

Doughlas and Olsen (1981)

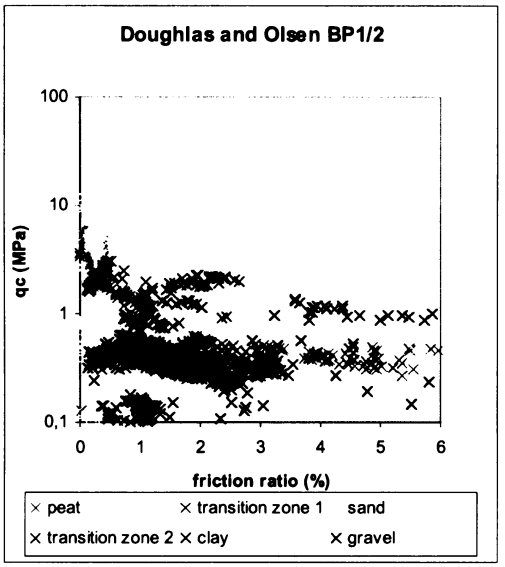

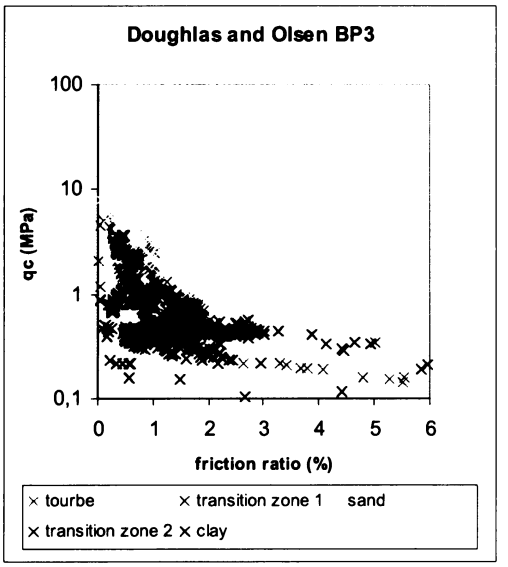

Janbu and Senneset (1984)

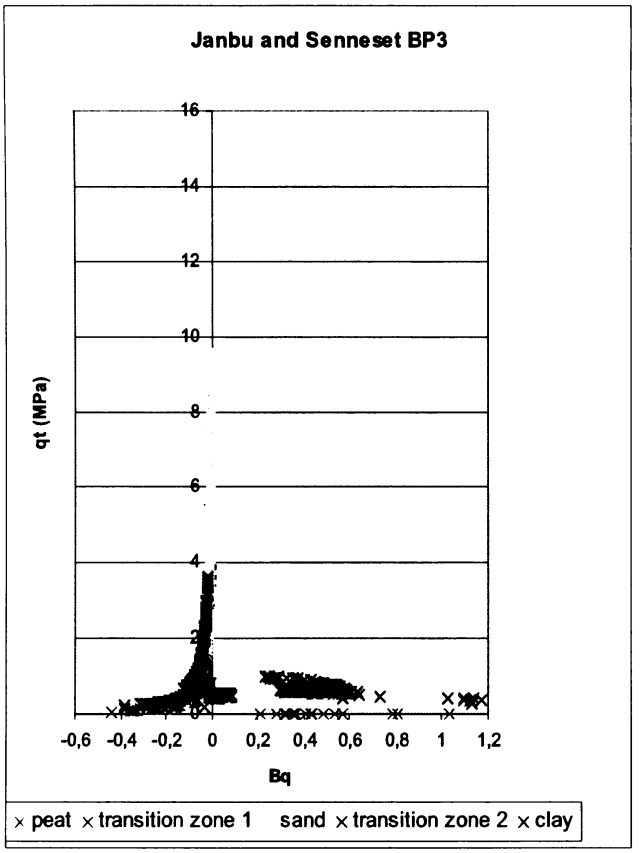

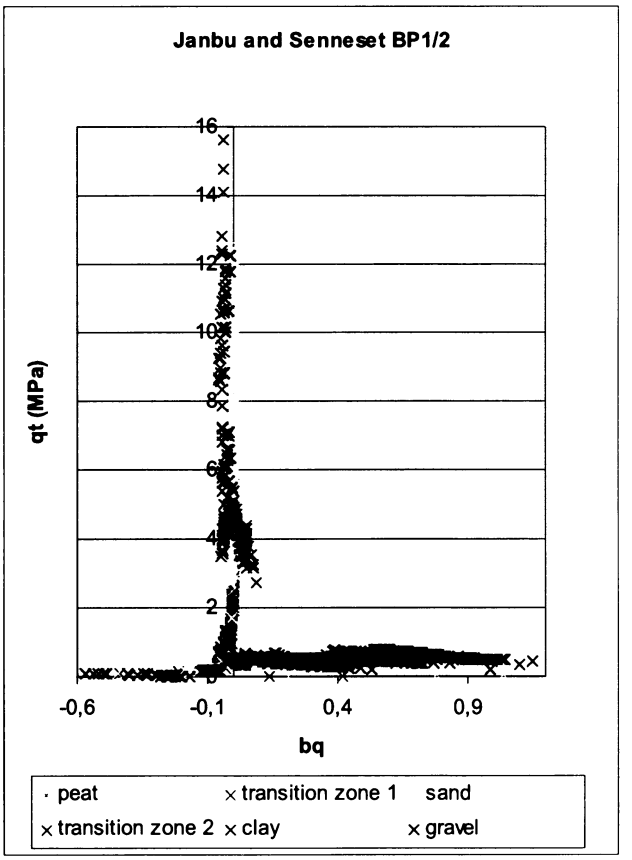

Robertson et al. 1986

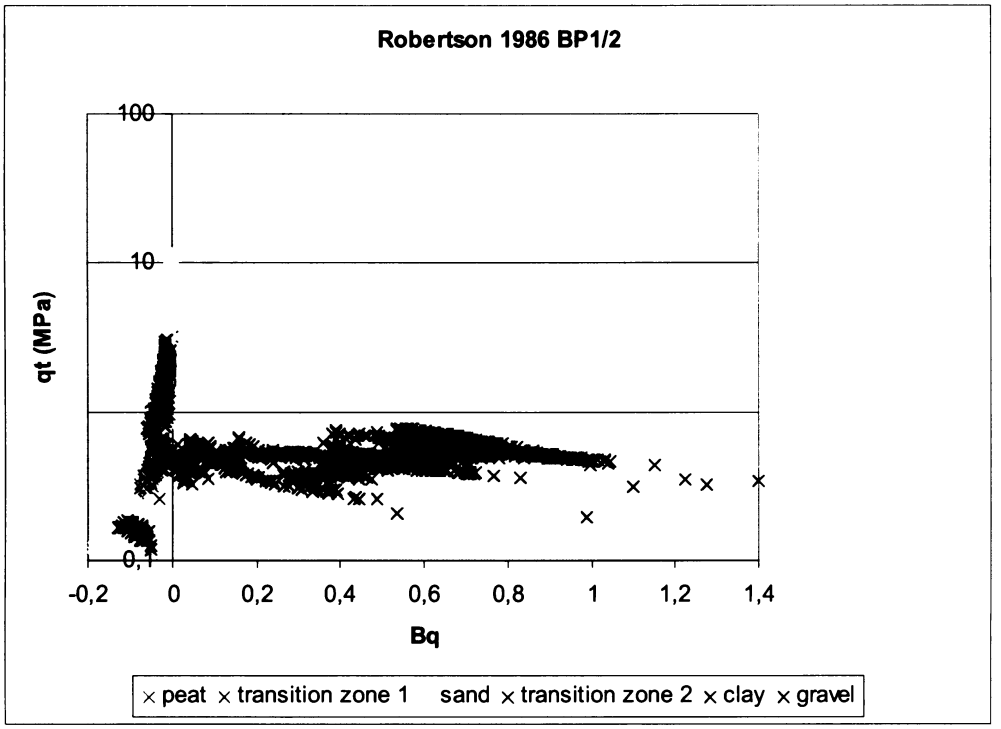

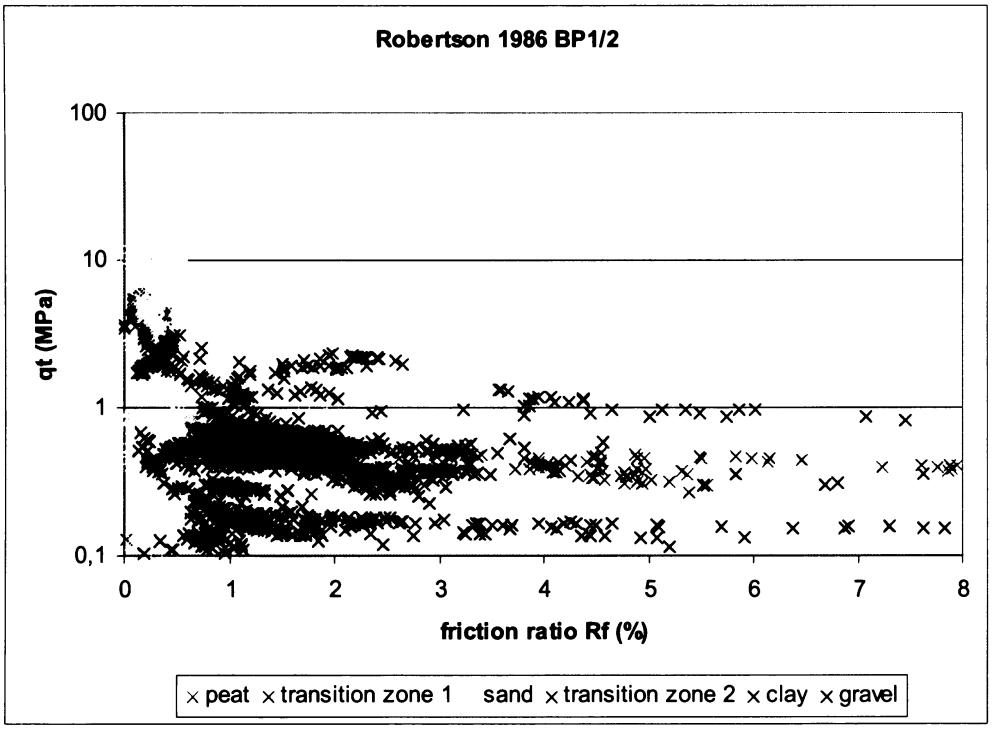

APPENDIX C

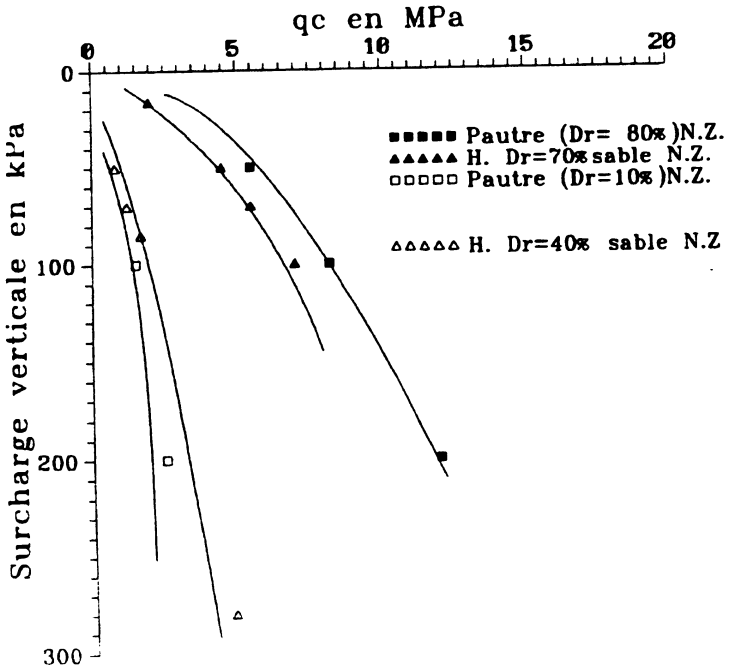

Figure C1. 1: Cone resistance versus effective stress for different sand densities (after Bougerra Hafid, 1997)

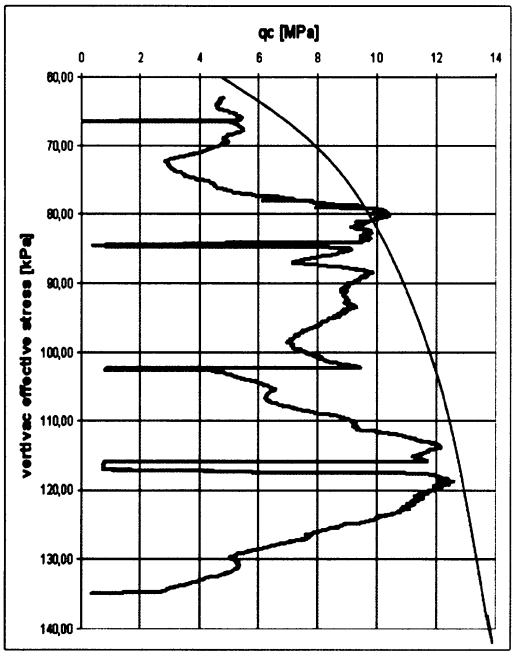

Figure C1. 2: A suggestion of an approximation curve (in blue), which could enable the sand relative density interpretation, although reliability of results obtained in this way is very doubtful.

APPENDIX D

Graphical Evaluation of liquefaction potential after Robertson (1990)

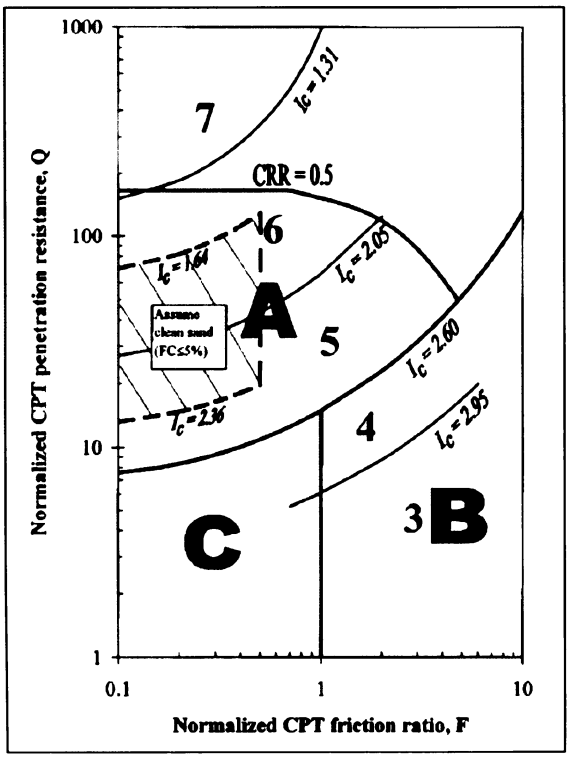

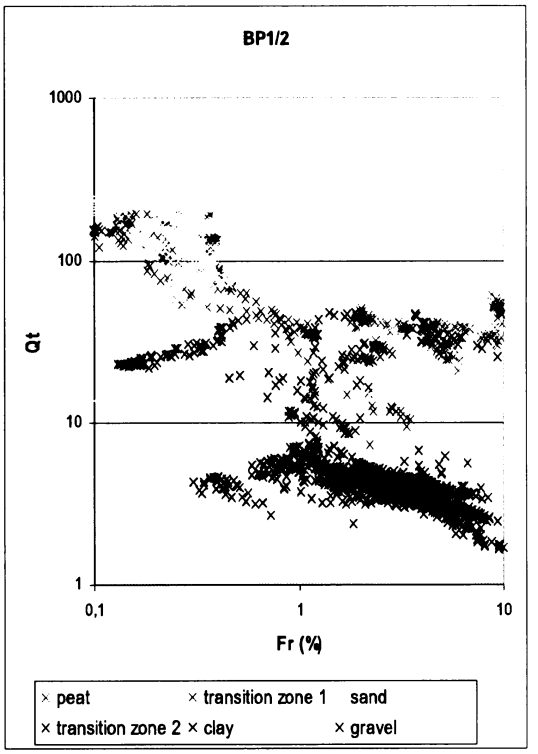

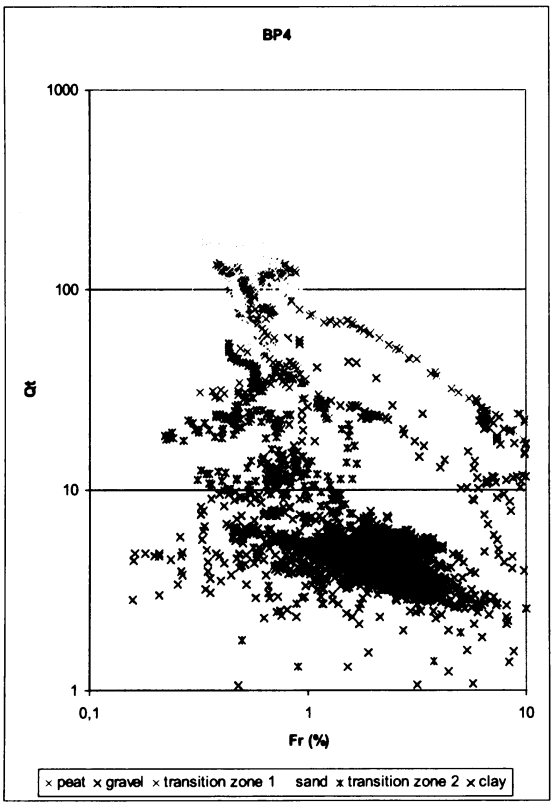

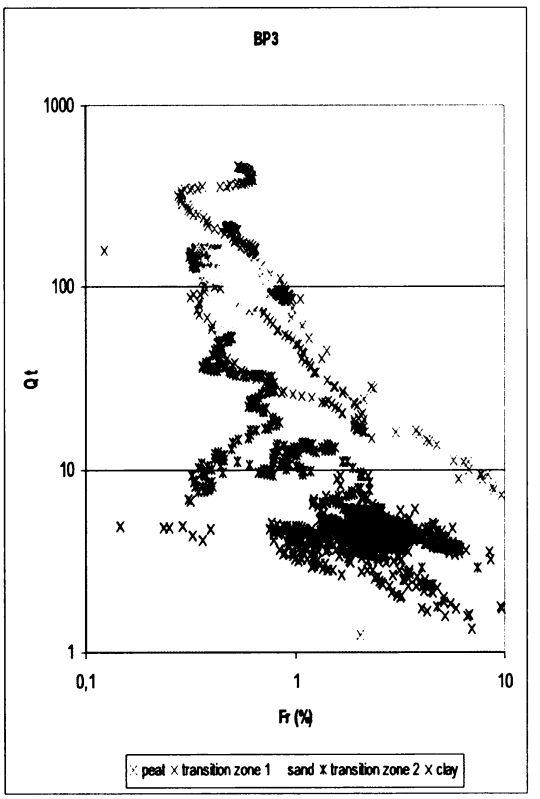

Graphical evaluation of liquefaction potential by comparison of qt versus Bq